Glia

WILEY

GLIA

RESEARCH ARTICLE OPEN ACCESS

The Alzheimer's Disease Gene *SORL1* Regulates Lysosome Function in Human Microglia

Swati Mishra[1,2] | Nader Morshed[3,4] | Sonia Beant Sidhu[1,2] | Chizuru Kinoshita[1,2] | Beth Stevens[3,4,5] | Suman Jayadev[2,6] | Jessica E. Young[1,2]

[1]Department of Laboratory Medicine and Pathology, University of Washington, Seattle, Washington, USA | [2]Institute of Stem Cell and Regenerative Medicine, University of Washington, Seattle, Washington, USA | [3]Boston Children's Hospital, F.M. Kirby Neurobiology Center, Boston, Massachusetts, USA | [4]Stanley Center for Psychiatric Research, Broad Institute of MIT and Harvard, Cambridge, Massachusetts, USA | [5]Howard Hughes Medical Institute, Boston, Massachusetts, USA | [6]Department of Neurology, University of Washington, Seattle, Washington, USA

Correspondence: Jessica E. Young (jeyoung@uw.edu)

Received: 14 June 2024 | **Revised:** 31 December 2024 | **Accepted:** 21 February 2025

Funding: This study was supported by NIA R01 AG062148, R01 AG AG080585 and an Alzheimer's Association Grant 23AARG-1022491 to J.E.Y., a Development Award to SM from the UW ADRC P30 AG066509, Alzheimer's Association "Endolysosomal Defects and Neuron-glia Crosstalk in Neurodegenerative Diseases" grant to B.S., and NIH training grants 5T32AG222-30 and 1F32AG079666-01 to N.M.

Keywords: Alzheimer's disease | hiPSC-derived microglia | lysosomes | phagocytosis | *SORL1*

ABSTRACT

The *SORL1* gene encodes the sortilin-related receptor protein SORLA, a sorting receptor that regulates endo-lysosomal trafficking of various substrates. Loss of function variants in *SORL1* are causative for Alzheimer's disease (AD) and decreased expression of SORLA has been repeatedly observed in human AD brains. *SORL1* is highly expressed in the central nervous system, including in microglia, the tissue-resident immune cells of the brain. Loss of SORLA leads to enlarged lysosomes in hiPSC-derived microglia-like cells (hMGLs). However, how SORLA deficiency contributes to lysosomal dysfunction in microglia and how this contributes to AD pathogenesis is not known. In this study, we show that loss of SORLA results in decreased lysosomal degradation and lysosomal enzyme activity due to altered trafficking of lysosomal enzymes in hMGLs. Phagocytic uptake of fibrillar amyloid beta 1–42 and synaptosomes is increased in SORLA-deficient hMGLs, but due to reduced lysosomal degradation, these substrates aberrantly accumulate in lysosomes. An alternative mechanism of lysosome clearance, lysosomal exocytosis, is also impaired in *SORL1*-deficient microglia, which may contribute to an altered immune response. Overall, these data suggest that SORLA has an important role in the proper trafficking of lysosomal hydrolases in hMGLs, which is critical for microglial function. This further substantiates the microglial endo-lysosomal network as a potential novel pathway through which *SORL1* may increase AD risk and contribute to the development of AD. Additionally, our findings may inform the development of novel lysosome and microglia-associated drug targets for AD.

1 | Introduction

Treatments for Alzheimer's disease (AD), a neurodegenerative disorder and the most common cause of dementia ("2023 Alzheimer's disease facts and figures," 2023), are few and do not alter the course of disease progression by more than several months. Hallmarks of AD include extracellular Amyloid-beta (Aβ) accumulation in senile plaques, intracellular aggregation of tau protein in neurofibrillary tangles, neurodegeneration and neuroinflammation. Microglia, tissue-resident phagocytes of the brain, are key effectors of pathogenic protein clearance and maintenance of neuronal health and brain homeostasis in general, positioning this brain cell type at the center of cellular responses in AD

pathogenesis and making it an attractive target for new AD therapies. Identification of AD risk genes highly expressed in microglia by genome-wide association studies (GWAS) further supports the idea that dysfunctional microglia may contribute to onset and/or progression of AD (Maninger et al. 2024; McQuade and Blurton-Jones 2019). Collective evidence from murine models and post-mortem human AD brain tissue has revealed that microglia migrate to and cluster around Aβ plaques (Akiyama et al. 1999; Bolmont et al. 2008; Itagaki et al. 1989; Meyer-Luehmann et al. 2008; Stalder et al. 1999) but are unable to eliminate these toxic deposits from the brain. One mechanism that may cause this defect is lysosome dysfunction in microglia. Abnormal lysosomes in microglia can negatively alter phagocytic and inflammatory responses (Iyer et al. 2022; Lancaster et al. 2021; Quick et al. 2023; Ren et al. 2022), functions known to cause neuroinflammation in AD, substantiating the need to investigate microglia-specific lysosomal pathways as therapeutic targets. Our previous work has shown that loss of the intracellular sorting receptor and potent AD risk gene, Sortilin-related receptor-1 (*SORL1*), that encodes the multidomain protein SORLA, results in enlarged lysosomes in hMGLs (Mishra 2024).

SORLA is a hybrid receptor that belongs to both the LDLR and the VPS10p receptor family. It interacts with the multi-protein assembly retromer and shuttles proteins between TGN, endosomes, and the cell surface (Fjorback et al. 2012; Jacobsen et al. 2001, 1996; Willnow and Andersen 2013; Yamazaki et al. 1996). In particular, retromer and its receptors, SORLA and the cation-independent mannose-6 phosphate receptor (CIMPR), function to traffic mature lysosomal hydrolases from the TGN via endosomes to lysosomes (Cui et al. 2019; Hasanagic et al. 2015; Nielsen et al. 2007). Genetic, epidemiological, and functional studies have now cumulatively and unequivocally established *SORL1* as a gene that increases the risk for AD, highlighting aberrant endo-lysosomal trafficking as an important pathway in AD pathogenesis (Holstege et al. 2017, 2023; Kunkle et al. 2017; Lambert et al. 2013; Rogaeva et al. 2007; Scheltens et al. 2021). Loss of SORLA expression has been observed in AD brains in the early stages of the disorder (Dodson et al. 2006; Scherzer et al. 2004; Thonberg et al. 2017). Studies investigating the role of SORLA in AD pathogenesis have extensively focused on neurons and revealed that loss of SORLA causes endo-lysosomal defects in neurons, specifically in endosomal recycling, autophagy, and lysosome function, ultimately resulting in increased secretion of toxic Aβ species and impaired synaptic activity in neurons (Andersen et al. 2022; Hung et al. 2021; Knupp et al. 2020; Lee et al. 2023; Mishra et al. 2023, 2022). While *SORL1* mRNA is highly expressed in microglia, even more so than in neurons and astrocytes (Lee et al. 2023; Olah et al. 2018; Zhang et al. 2016), the impact of loss of SORLA function specifically in microglia is not well-studied, rendering our understanding of the role of SORLA in AD risk incomplete at best. Understanding cell-type-specific functions of AD risk genes, including SORLA, is imperative in understanding the etiology and pathogenesis of the disease and in developing rational therapeutic approaches for AD.

In this study, we investigated how SORLA deficiency affects lysosomal function in hiPSC-derived microglia-like cells (hMGLs). We used quantitative flow cytometry, immunocytochemistry, and functional enzymatic and cellular assays to reveal that *SORL1* KO hMGLs show decreased lysosomal degradation and reduced lysosomal enzymatic activity due to impaired trafficking of lysosomal enzymes from the trans-Golgi network (TGN) to lysosomes. We show that the main retromer cargo that functions with *SORL1* to traffic lysosomal enzymes, CIMPR, has reduced expression in *SORL1*-deficient hMGLs and reduced co-localization with enzymes in lysosomes. This impairment in enzyme trafficking leads to inefficient lysosomal degradation and accumulation of phagocytosed fibrillar Aβ 1–42 and synaptosomes in lysosomes. Impaired degradation leads to lysosomal stress and could prompt cells to rid themselves of undigested cargo via other mechanisms (Domingues et al. 2024; Wang, Telpoukhovskaia, et al. 2018; Zhong et al. 2023). We tested lysosomal exocytosis (LE), a secretory pathway through which microglia release lysosomal enzymes, cargo, and inflammatory cytokines into the extracellular environment and found that this process is also altered in *SORL1* KO hMGLs. Overall, our data show that *SORL1* regulates lysosomal homeostasis in human microglia. Loss of normal *SORL1* function leads to mis-trafficking of lysosomal enzymes and impairment of critical lysosomal functions, including substrate degradation and LE. This data, along with recent work describing a role of SORLA in sorting neuroimmune receptors (Ovesen et al. 2024), adds to a growing body of work highlighting *SORL1* and related pathways as novel therapeutic targets for AD.

2 | Materials and Methods

2.1 | Cell Lines

Cell lines generated by CRISPR/Cas9 gene editing technology: Isogenic cell lines with loss of *SORL1* were generated using CRISPR/Cas9 genome editing, as described in our previous study (Knupp et al. 2020). Briefly, cell lines were generated from our previously published and characterized CV background human induced pluripotent stem cell line (Young et al. 2015). This cell line is male and has an APOE ε3/ε4 genotype (Levy et al. 2007). Genome-edited lines were generated using published protocols (Young et al. 2018). Briefly, guide RNAs (gRNAs) to *SORL1* were generated using the Zhang Lab CRISPR Design website at MIT (http://zlab.bio/guide-design-resources) and selected to minimize off-target effects. gRNAs were cloned into the vector px458 that co-expresses the Cas9 nuclease and GFP, and hiPSCs were electroporated with the plasmid. Electroporated hiPSCs were FACS sorted for GFP, plated in 10 cm plates at a clonal density (~1×10^4 cells/plate), and allowed to grow for roughly 2 weeks. Colonies were picked into 96 well plates and split into two identical sets. One set was analyzed for sequence information by Sanger sequencing, and one set was expanded for cell line generation. Four clones were chosen for experiments reported in this publication. Two wild-type (WT) clones and two *SORL1* KO clones were selected. Sequencing data for all cell lines were confirmed by measuring protein expression using western blot techniques, as described in our previous studies (Knupp et al. 2020; Mishra et al. 2023, 2022). All four clones were shown to have normal karyotypes. Authentication by Sequencing data confirming CV cell lines by the presence of a SNP unique

to this genetic background is also described in our previous studies (Knupp et al. 2020; Mishra et al. 2023, 2022). All cell lines are routinely karyotyped by Diagnostic Cytogenetics Inc. (Seattle, WA) and tested for mycoplasma (MycoAlert). CRISPR/Cas9 gRNA, ssODN, and Primer Sequences gRNA:ATTGAACGACATGAACCCTC ssODN: GGGAATT GATCCCTATGACAAACCAAATACCATCTACATTGAA CGACATGAACCCTCTGGCTACTCCACGTCTTCCGA GTACAGATTTCTTCCAGTCCCGGGAAAACCAGGAAG Forward primer: ctctatcctgagtcaaggagtaac Reverse primer: ccttccaattcctgtgtatgc PCR amplifies a 458 bp sequence.

2.2 | Differentiation of Human iPSCs Into Microglia Like Cells (hMGLs)

hiPSCs were differentiated into hMGLs as previously described with some modifications (McQuade et al. 2018). Briefly, hiPSCs were plated in mTESR plus medium supplemented with ROCK Inhibitor (Y-27632; # A3008; Apex Bio) on Matrigel (Growth factor reduced basement membrane matrix; # 356231; Corning)-coated 6-well plates (#657160; CELLSTAR). To begin hematopoietic progenitor differentiation, hiPSC aggregates were plated at a density of 20–40 aggregates per well of a 6-well plate, which resulted in the attachment of ~10 colonies per well of a 6-well plate for all the cell lines. In our hands, this plating density protocol resulted in maximum yield and efficient differentiation of HPCs from hiPSCs without the generation of cell debris. On day 0, mTESR plus medium was replaced with STEMdiff Hematopoietic Supplement A medium from the STEMdiff Hematopoietic kit (# 05310; STEMCELL technologies). On Day 3, when colonies became flattened, medium was replaced with STEMdiff Hematopoietic Supplement B medium from the STEMdiff Hematopoietic kit (# 05310; STEMCELL technologies). Cells remained in this medium for seven additional days. By Day 12, non-adherent hematopoietic progenitor cells (HPCs) coming off from the flattened colonies were harvested by removing medium. Any remaining HPCs/floating cells were collected by gentle PBS washes. At this point, HPCs were either frozen using Bambanker cell freezing medium (#BBH01; Bulldog-Bio) or plated at a density of 0.2 million cells per well of a Matrigel-coated 6-well plate in microglia differentiation medium for 24 days. Microglia differentiation medium comprised DMEM-F12 (#11039047; Thermo Fisher Scientific), Insulin-transferrin-selenite (#41400045; Thermo Fisher Scientific), B27 (# 17504-044; Thermo Fisher Scientific), N2 (# 17502-048; Thermo Fisher Scientific), Glutamax (# 35050061; Thermo Fisher Scientific), nonessential amino acids (# 11140050; Thermo Fisher Scientific), monothioglycerol (# M1753; Sigma), Insulin (# I2643; Sigma) freshly supplemented with TGF-β (#130-108-969, Miltenyi), IL-34 (# 200-34; Peprotech) and M-CSF (#PHC9501; Thermo Fisher Scientific). On day 24, this medium was supplemented with CD200 (#C311; Novoprotein) and CX3CL1 (#300-31; Peprotech) for maturation of microglia. Cells remained in this medium for 8 days. On Day 32, microglia differentiation was complete, and these cells were plated on poly-l-lysine (#P6282; Sigma; 100 μg/mL)-coated coverslips (12 mm diameter, #1760-012; cglifesciences) in a 24-well plate for immunocytochemistry with appropriate antibodies or poly-l-lysine-coated 48-well plates for flow cytometry.

2.3 | Meso-Scale Discovery (MSD) V-PLEX Platform to Measure Extracellular Levels of Cytokines in hMGLs

Pro-inflammatory cytokines in the media were measured using the Proinflammatory Panel 1 (human) kit (#K15049D; MSD V-PLEX MULTI-SPOT assay System; MesoScale Diagnostics). For this assay, hMGLs were plated at a density of 100,000 cells/well of a Matrigel-coated 96 well plate and allowed to settle for 24 h. Cells were then treated with 20 ng/mL IFNγ or 100 ng/mL lipopolysaccharide (LPS) for 24 h. Conditioned media were harvested at the end of 24 h and stored at −80°C until use. A total of 50 μL of media was used to run the MSD V-plex assay as per the manufacturer's protocol, and the MSD Quick plex SQ120 instrument was used to detect analytes. This MSD V-Plex Proinflammatory Panel detects a panel of Pro-inflammatory cytokines including IL-1β, IL-6, IL-8, IFN-γ, TNF-α, IL-13, IL-2, IL-4, IL-10, and IL-12p70, known to be altered in AD patients (Park et al. 2020; Taipa et al. 2019).

2.4 | ELISAs to Measure Extracellular Levels of Cytokines in hMGLs

Extracellular levels of the cytokines, IL-6, and IL-1β were measured using the human IL-6 ELISA kit (#ab178013, abcam) and the human IL-1β ELISA kit (#BMS224-2; Thermo Fisher Scientific). To test the secretion of these cytokines upon activation with the LE activator, calcimycin, cells were treated with 1 μM calcimycin for 24 h; extracellular levels (media) and intracellular levels (lysates) of IL-1β and IL-6 were measured using the ELISA kits described above.

2.5 | In Vitro Fibrillation of Amyloid-β (1–42) (fAβ)

HiLyte Fluor 647 beta-amyloid (1–42) (# AS-64161, Anaspec) was fibrillized as described previously (Amos et al. 2017). Briefly, Aβ-42 was resuspended in sterile 1X PBS to generate a final concentration of 100 μM, placed at 37°C for 5 days for fibrillization, aliquoted, and stored at −80°C.

2.6 | Phagocytosis of Fibrillar Amyloid-β (1–42) and Oligomeric Amyloid-β (1–42)

To measure phagocytosis of fAβ by hMGLs, Aβ labeled with a fluorophore, HiLyte Fluor 647 beta-amyloid (1–42) (# AS-64161, Anaspec) was fibrillized as described above and commercially available Oligomeric Aβ (1–42) (# SPR-488; Stress Marq Biosciences) was labeled with the Alexa Fluor 647 fluorophore using the Microscale Protein Labeling Kit (#A30009; Thermo Fisher Scientific). fAβ-647 (fAβ) and Oligomeric Aβ-647 (oAβ) were used for the phagocytosis assay. hMGLs were plated at a density of 100,000 cells per well of a poly-l-lysine (100 μg/mL)-coated 48-well plate. Cells were treated with this fAβ (0.1 μM) and oAβ (10 μg/mL) for 30 min, 5 h, and 24 h. At the end of each time point, cells were washed with 1X PBS and harvested using Accutase. Intracellular fluorescence of fAβ and oAβ was

measured using flow cytometry. Data were analyzed using Flow Jo software. Fluorescence measured at 30 min indicates uptake efficiency, and the longer time points can either indicate sustained phagocytic capacity of hMGLs or accumulation of undegraded substrates in the lysosomes. As an additional method to test phagocytosis of fibrillar Aβ by hMGLs, the phagocytosis assay was performed as described above. Subsequently, phagocytosis was examined using immunocytochemistry with cells fixed with 4% PFA in PBS for 10 min and imaged using the Leica SP8 microscope.

2.7 | Phagocytosis of Synaptosomes

To measure phagocytosis of synaptosomes, a phagocytosis assay was performed as previously described with some modifications (Beeken et al. 2022). Briefly, synaptosomes were harvested from Wildtype hiPSC-derived neurons using Syn-PER Synaptic Protein Extraction Reagent (# 87793; Thermo Fisher Scientific). A total of 3 mL of Syn-PER reagent was added to a 100mm tissue culture dish of neurons (~30 M cells), cells were harvested by scraping and centrifuged at 1200 g for 10 min. The supernatant was collected and centrifuged at 15,000 *g* for 20 min at 4°C, and the pellet, which is the synaptosomes (crude synaptosome extraction), was either resuspended in Krebs ringer solution (with 1X protease inhibitor) and frozen at −80°C or labeled with CM-Dil cell tracker dye (final concentration 3 μM) as per the manufacturer's instructions (#C7000; Thermo Fisher Scientific). CM-Dil labeled synaptosomes were added to hMGLs plated on poly-l-lysine-coated 48-well plates, and cells were harvested at the end of different time points including 30 min, 5 h, and 24 h. The intracellular fluorescence intensity of CM-Dil labeled synaptosomes was measured using flow cytometry as a readout of phagocytosis of synaptosomes by hMGLs. To further confirm phagocytosis of synaptosomes by hMGLs, a phagocytosis assay was performed as described above, followed by immunocytochemistry with cells fixed with 4% PFA in PBS for 10 min and imaged using the Leica SP8 microscope.

2.8 | Uptake Assays

To test the uptake of FITC-Dextran (0.5 mg/mL; #46944-100MG-F; Millipore Sigma) and Transferrin from Human Serum, Alexa Fluor 647 Conjugate (25 μg/mL; #T23366; Thermo Fisher Scientific), hMGLs were treated with each substrate for 2 h in a cell culture incubator, and fluorescence intensity was measured using flow cytometry. Analysis was performed using Flow Jo software. To test uptake of BSA-594 (10 μg/mL; #A13101; Thermo Fisher Scientific), cells were treated with this reagent for 30 mins, washed thrice and mean fluorescence intensity was measured using flow cytometry.

2.9 | Western Blotting

For western blot analysis, cell lysates were harvested from hMGLs using RIPA protein lysis buffer (#20-188; Millipore) containing 1X protease and 1X phosphatase inhibitors (#PI78443; Thermo Fisher Scientific). Total protein concentration was quantified using the Pierce BCA assay kit (#23225; Thermo Fisher Scientific). Briefly, 10–20 μg of protein lysates were run on 4%–20% Mini-PROTEAN TGX Precast Protein Gels (#4561096; Biorad) and transferred to PVDF membranes. Membranes were blocked with 5% w/v non-fat dry milk in 1X PBS (blocking buffer), washed with 1X PBS with 0.05% tween 20 (PBST) and incubated overnight at 4°C with the following primary antibodies diluted in 0.2% sodium azide + 5% BSA in 1X PBS: Sortilin-related receptor 1 (SORLA) at 1:1000 (# ab190684; abcam); Mouse monoclonal anti-Actin (clone A4) (#MAB1501; Millipore Sigma) at 1:2000; Rabbit monoclonal anti-HEXB (#ab140649; abcam); Goat anti-Cathepsin B (#ab214428; abcam); Mouse monoclonal anti-Cathepsin D (#ab6313; abcam) and Rabbit monoclonal anti-LAMP1 (#9091S; Cell signaling); Rabbit Polyclonal P2Y6 receptor (#APR-106; Alomone labs); Human TREM2 (#MAB17291; R&D); and Anti-M6PR (cation independent) antibody [EPR6599] (#ab124747; Abcam). Membranes were then washed with PBST, incubated in corresponding HRP-conjugated secondary antibodies for 1 h. The following secondary antibodies were used: Goat anti-Mouse IgG (H + L) Secondary Antibody HRP (#31430; Thermo Fisher Scientific) Goat anti-Rabbit IgG (H + L) Secondary Antibody HRP (# 31460; Thermo Fisher Scientific) and Donkey anti-goat IgG (H + L) Secondary Antibody (#A15999; ThermoFisher Scientific). Membranes were then washed thrice with PBST, probed with either Clarity Western ECL substrate (#1705061; Biorad) or Clarity Max Western ECL Substrate, and scanned using an Odyssey Clx imaging system (Li-Cor) to detect bound proteins on membranes. To normalize protein levels in the media, ponceau staining was used.

2.10 | Lysosomal Degradation Assay

Lysosomal degradation in hMGLs was measured using DQ-BSA (#12051; Thermo Fisher Scientific) which is a fluorogenic substrate for proteases and fluoresces only when degraded in lysosomes. For this assay, hMGLs were plated at a density of 100,000 cells per well of a poly-l-lysine-coated 48-well plate. A pulse-chase experiment was performed wherein hMGLs were treated with 20 μg/mL DQ-BSA for 20 min. At the end of this timepoint, cells were washed with 1X PBS and cultured in complete microglia medium for 30 min, 2 h, and 5 h. At the end of each timepoint, cells were washed with 1X PBS and harvested using accutase. Intracellular fluorescence intensity of DQ-BSA was measured using flow cytometry, and data was analyzed using FlowJo software. Altered fluorescent intensity of DQ-BSA was measured as a readout of altered lysosomal degradation. As an additional method to examine lysosomal degradation, we performed pulse-chase experiment as described above and immunocytochemistry (cells fixed after 2 h) after treating cells with DQ-BSA, and intracellular fluorescence intensity was noted as a readout of lysosomal degradation. Treatment with the lysosomotropic agent chloroquine (50 μM) was used as a negative control for both experiments.

2.11 | Lysosomal Enzyme Activity Assays

To measure lysosomal enzyme function, lysosomal enzyme activity assays were performed. For hMGLs generated using a protocol based on McQuade et al. (2018), 200,000 hMGLs were plated per well of a poly-l-lysine-coated 48-well plate. Cells were allowed to settle for 24 h. Specifically, the enzyme activity of lysosomal enzymes, Cathepsin D (#ab65302; abcam), Cathepsin B (#ab 65300; abcam) and Hexosaminidase

B (#MET-5095; Cell Bio labs) was measured as per the manufacturers protocol.

2.12 | Immunocytochemistry

hMGLs were seeded at a density of 200,000 cells per well of a poly-l-lysine-coated 24-well plate on glass coverslips. After 2 days in culture, cells were fixed in 4% paraformaldehyde (PFA, Alfa Aesar, Reston, VA) for 10 min. Cells were washed with 1X PBS + 0.05% tween 20 detergent, incubated in blocking buffer containing 5% goat (#005-000-121; Jackson ImmunoResearch) or donkey serum (#017-000-121; Jackson ImmunoResearch), permeabilized using 0.1% Triton X-100 (Sigma Aldrich, St Louis, MO) for 15 min at room temperature, and then incubated in a primary antibody dilution in blocking buffer overnight at 4°C. Cells were then washed three times with PBS + 0.05% tween 20 and incubated with a secondary antibody dilution in blocking buffer for 1 h at room temperature in the dark. Cells were then washed with 1X PBS with tween 20 and mounted on glass slides with ProLong Gold Antifade mountant with DAPI (#P36931; Thermo Fisher Scientific). To measure surface expression, cells were not permeabilized. Surface expression was reported as fluorescence intensity of surface proteins normalized to cell area as measured by the Image J software.

2.13 | Colocalization Analysis

To investigate the colocalization of lysosomal enzymes with the TGN or lysosomes, hMGLs were plated in a 24-well plate with 12 mm diameter coverslips, allowed to settle for 48 h, and fixed with 4% PFA in PBS. Immunocytochemistry was performed using primary antibodies against lysosomal enzymes, Cathepsin B, Cathepsin D, HEXB, Cation-Independent Mannose-6-phosphate receptor (CIMPR) and TGN marker, TGN38, and late endosomal and lysosomal marker, LAMP1. Cells were co-labeled for either TGN and lysosomal enzymes or LAMP1 and lysosomal enzymes. For the lysosomal enzymes and CIMPR, the same antibodies were used for both immunocytochemistry and western blotting. To label TGN and lysosomes, TGN38 (B6) mouse monoclonal antibody (#166594; SantaCruz) and LAMP1 mouse monoclonal antibody (#sc20011; Santacruz) were used. A minimum of 10 fields of confocal images were captured using the Leica SP8 microscope. Images were analyzed using ImageJ software. Median filtering was used to remove noise from images, and Otsu thresholding was applied to all images. Colocalization was quantified using the JACOP plugin in ImageJ software and presented as Mander's correlation coefficient.

2.14 | Confocal Microscopy and Image Processing

All microscopy and image processing were performed under blind conditions. Z stack images were acquired using the Leica TCS SP8 confocal laser microscope with a 63x/1.40 oil lens (Leica Microsystems) and modified/processed using Leica Application Suite X 3.5.5.19976 with LIGHTNING adaptive deconvolution (Leica Microsystems). A total of 10–20 fields were imaged per experiment per clone, which included a total of 50–100 cells. For some experiments, images were processed further using ImageJ software (Schindelin et al. 2012).

2.15 | Measurement of Surface LAMP1 Expression

To measure surface LAMP1 expression, hMGLs were plated at a density of 100,000 cells per well of a 48-well plate and allowed to settle for 48 h. Cells were then either treated with the calcium ionophore, calcimycin (#C4403; Sigma) +4 mM $CaCl_2$ + 0.1% BSA in PBS to stimulate LE or 0.1%BSA in PBS as control and placed in the cell culture incubator for 30 min. Next, cells were placed on ice for 15 min and treated with cold Mouse monoclonal antibody against LAMP1 (#328611; Biolegend) specific to the N-terminal luminal epitope of the antigen for an hour on ice. Cells were then washed with 1X PBS and either treated with Accutase and used for flow cytometry or fixed with 4% PFA in PBS for 5 min and used for immunocytochemistry. Surface expression of LAMP1 was presented as fluorescence measured by flow cytometry and FlowJo software or immunocytochemistry and ImageJ software.

2.16 | Quantification and Statistical Analysis

All data presented in this study represent multiple hiPSC clones. This includes two clones for WT hMGLs and two clones for *SORL1* KO hMGLs. All data represent at least six independent experiments (called replicates) per clone. Experimental data were tested for normal distributions using the Shapiro–Wilk normality test. Normally distributed data were analyzed using parametric two-tailed unpaired *t* tests, one-way ANOVA tests, or two-way ANOVA tests. Significance was defined as a value of $p < 0.05$. All statistical analysis was completed using GraphPad Prism software.

3 | Results

3.1 | Loss of *SORL1* Decreases Lysosomal Degradation in hMGLs

We have previously shown that *SORL1* KO hMGLs have enlarged lysosomes, indicating lysosome dysfunction and stress (Mishra 2024). We hypothesized that lysosomal dysfunction would impair the degradative capacity of this organelle. To test this hypothesis, we generated WT and *SORL1* KO HPCs and hMGLs using a previously published protocol (McQuade et al. 2018) with minor modifications (described in Section 2). HPC-specific expression was confirmed in WT and *SORL1* KO HPCs using immunostaining with the HPC marker CD43, and microglia-specific expression was demonstrated by immunostaining with the microglia markers IBA1 and CX3CR1. Loss of *SORL1* did not alter differentiation of hiPSCs into HPCs and hMGLs (Figure S1). To determine if overall proteolytic lysosomal degradation is affected, we performed a pulse-chase assay with DQ-Red-BSA, a fluorogenic substrate that fluoresces only upon degradation (Marwaha and Sharma 2017) (Figure 1A). Mean fluorescence intensity (MFI) was measured by flow cytometry as a readout of lysosomal degradation. Both WT and *SORL1* KO hMGLs showed an increase in MFI over a period of 2 h, suggesting our hiPSC-derived microglia were capable of lysosomal degradation in vitro, although *SORL1*

KO hMGLs demonstrated reduced MFI of DQ-Red-BSA as compared to WT hMGLs at all time points tested (Figure 1B), suggesting either decreased uptake and/or degradation of the substrate. Inhibiting lysosome proteolysis with the lysosomotropic reagent chloroquine abrogated lysosomal degradation of DQ-Red-BSA in both WT and *SORL1* KO hMGLs (Figure 1B),

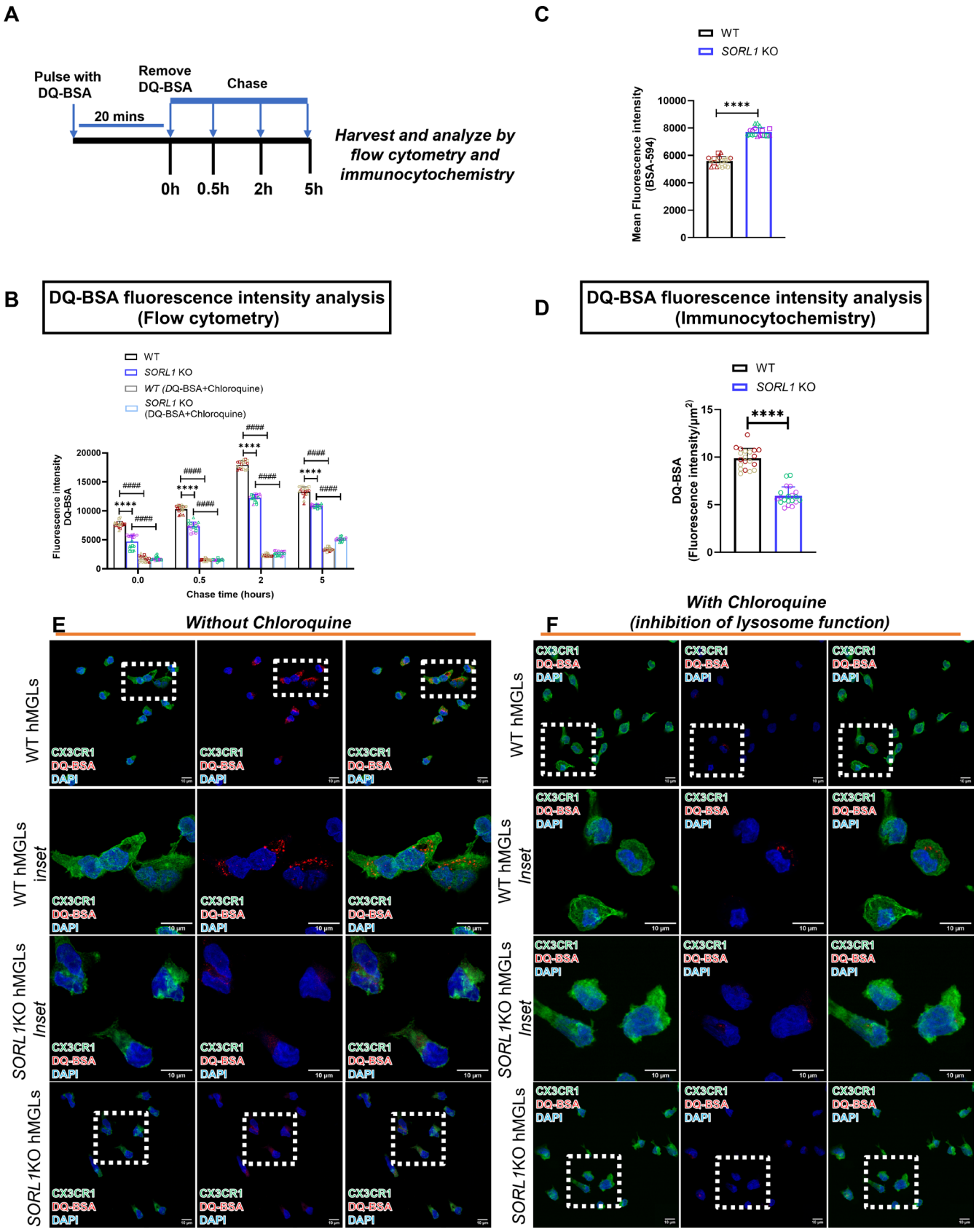

FIGURE 1 | Legend on next page.

FIGURE 1 | Loss of *SORL1* results in decreased lysosomal degradation in hMGLs. (A) Schematic illustrating experimental design using DQ-BSA, a fluorogenic protease substrate that fluoresces only upon lysosomal degradation by proteases. (B) A pulse chase experiment performed with WT and *SORL1* KO hMGLs and mean fluorescence intensity (MFI) measured using flow cytometry. *SORL1* KO hMGLs show decreased MFI of DQ-BSA at all timepoints, indicating decreased lysosomal degradation. The lysosomotropic agent chloroquine, which inhibits lysosomal degradation, was used as a control. Chloroquine treatment shows decreased lysosomal degradation of DQ-BSA in both WT and *SORL1* KO hMGLs. (C) Flow cytometry showing increased MFI of BSA-594 in *SORL1* KO hMGLs relative to WT hMGLs, suggestive of increased uptake of BSA in hMGLs with loss of *SORL1*. (D–F) Immunocytochemistry of hMGLs treated with DQ-BSA using the experimental design in (A), cells fixed for 2 h and labeled with the microglia marker, CX3CR1 showing decreased lysosomal degradation in *SORL1* KO hMGLs as compared to WT hMGLs, validating results obtained from the experiments using flow cytometry. Similar to the flow cytometry experiment, chloroquine was used as a control and showed decreased MFI in both WT and *SORL1* KO hMGLs, indicating reduced lysosomal degradation Quantification of fluorescence intensity of DQ-BSA using Image J software after immunocytochemistry with the microglia marker CX3CR1 and treatment with DQ-BSA. (E and F). Two isogenic clones per genotype (WT and *SORL1* KO) and nine independent replicates (three differentiations and three technical replicates per differentiation) per clone per genotype ($N = 18$ independent replicates) were used for these experiments. Data represented as mean ± SD and analyzed using parametric two-tailed unpaired t test and two-way ANOVA with Tukeys multiple comparison test. Significance while comparing WT to *SORL1* KO hMGLs was defined and depicted as a value of $^{*}p < 0.05$, $^{**}p < 0.01$, $^{***}p < 0.001$, and $^{****}p < 0.0001$, ns = not significant, and while comparing different treatments of each genotype was defined and depicted as a value of $\#p < 0.05$, $\#\#p < 0.01$, $\#\#\#p < 0.001$, and $\#\#\#\#p < 0.0001$, ns = not significant.

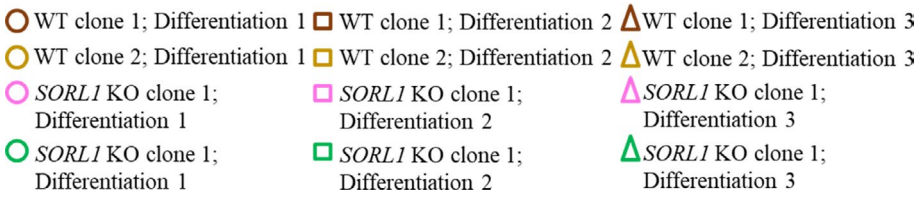

validating our degradation assays. To test if decreased fluorescence intensity of DQ-BSA observed in *SORL1* KO hMGLs is caused by decreased uptake of the reagent, we tested the uptake of a proxy reagent, BSA conjugated to a red fluorophore (BSA-594), which also undergoes pinocytic uptake similar to DQ-BSA. A proxy reagent was used because short-term uptake of DQ-BSA cannot be measured directly since it fluoresces only upon reaching the lysosomes. Interestingly, we observed an increased uptake of BSA-594 in *SORL1* KO hMGLs as compared to WT hMGLs (Figure 1C). To further corroborate our data, we performed an uptake assay with a general pinocytosis marker, FITC-Dextran, and observed a similar trend in *SORL1* KO hMGLs (Figure S4A). Together, this data suggest that *SORL1* KO hMGLs have reduced lysosomal degradation of DQ-Red-BSA rather than reduced uptake of DQ-BSA. To further confirm our findings with an independent method, we performed a pulse-chase assay and immunocytochemistry. We incubated hMGLs with DQ-Red-BSA similar to the experiment described above, and cells were fixed after 2 h. Immunocytochemistry was performed to label cells with the microglia marker CX3CR1. In support of our hypothesis, we observed decreased lysosomal degradation in *SORL1* KO hMGLs as compared to WT hMGLs (Figure 1D–F). Overall, our data demonstrated that loss of *SORL1* causes reduced lysosomal degradation in hMGLs.

3.2 | Loss of *SORL1* Decreases Intracellular Lysosomal Enzyme Activity in hMGLs

Next, we investigated intracellular lysosomal enzyme activity as a potential cause for altered lysosomal degradation observed in *SORL1* KO hMGLs. We tested intracellular enzyme activity of three key lysosomal enzymes, Beta-hexosaminidase subunit beta (HEXB), Cathepsin D (CTSD), and Cathepsin B (CTSB). All three enzymes are highly expressed in microglia; CTSD and CTSB have been proposed to degrade Aβ and tau, and altered expression of all three enzymes has been observed in AD (Cermak et al. 2016; Di Spiezio et al. 2021; Hamazaki 1996; Ii et al. 1993; Kenessey et al. 1997; Kuil et al. 2019; Sierksma et al. 2020; Sun et al. 2008; Whyte et al. 2022). Furthermore, altered expression or activity of these enzymes causes significant lysosome dysfunction and affects Aβ deposition in mouse brains (Keilani et al. 2012; Koike et al. 2000; Oberstein et al. 2021; Suire et al. 2020; Suzuki et al. 2022; Wang et al. 2012). Depletion of *SORL1* resulted in reduced lysosomal enzyme activity of HEXB, CTSD, and CTSB (Figure 2A–C) without altering protein expression in *SORL1* KO hMGLs relative to WT hMGLs (Figure 2D–I). Chloroquine treatment was used as a negative control in enzyme activity assays and, as expected, resulted in decreased lysosomal enzyme activity for all the enzymes (Figure 2A–C). To further confirm our hypothesis and account for potential heterogeneity introduced by microglia differentiation protocols, we tested lysosomal enzyme activity in hiPSC-derived microglia generated using a different protocol (Dolan et al. 2023). Characterization of these hMGLs showed no difference in expression of microglia-specific markers between WT and *SORL1* KO cells (Figure S2A). Using these hMGLs, we independently confirmed reduction in intracellular CTSD activity (Figure S2B), validating our hypothesis that loss of *SORL1* results in reduced lysosomal enzyme activity. Overall, our data suggest that decreased lysosomal enzyme activity, rather than changes in overall lysosomal protein expression, contributes to the reduction in lysosomal degradation observed in *SORL1* KO hMGLs. Our results are concordant with a recent study that showed no difference in mRNA and protein expression of CTSD, CTSB, and HEXB in *SORL1* KO hMGLs using mRNA-sequencing and TMT proteomics (Lee et al. 2023). Furthermore, lysosomal phenotypes due to *SORL1* deficiency are not due to differences between in vitro differentiation protocols.

3.3 | Loss of *SORL1* Results in Altered Trafficking of Lysosomal Enzymes in hMGLs

Newly synthesized lysosomal enzymes are transported from the trans Golgi network (TGN) to the lysosome using either a mannose-6-phosphate (M6P)-dependent pathway primarily regulated by Cation Independent Mannose-6-phosphate receptor (CIMPR) and the multi-protein complex retromer (Arighi et al. 2004; Braulke and Bonifacino 2009; Cui et al. 2019) or in an M6P-independent pathway in which enzymes are directly targeted to the lysosome (Gauthier et al. 2024; Hasanagic et al. 2015). SORLA can bind to the

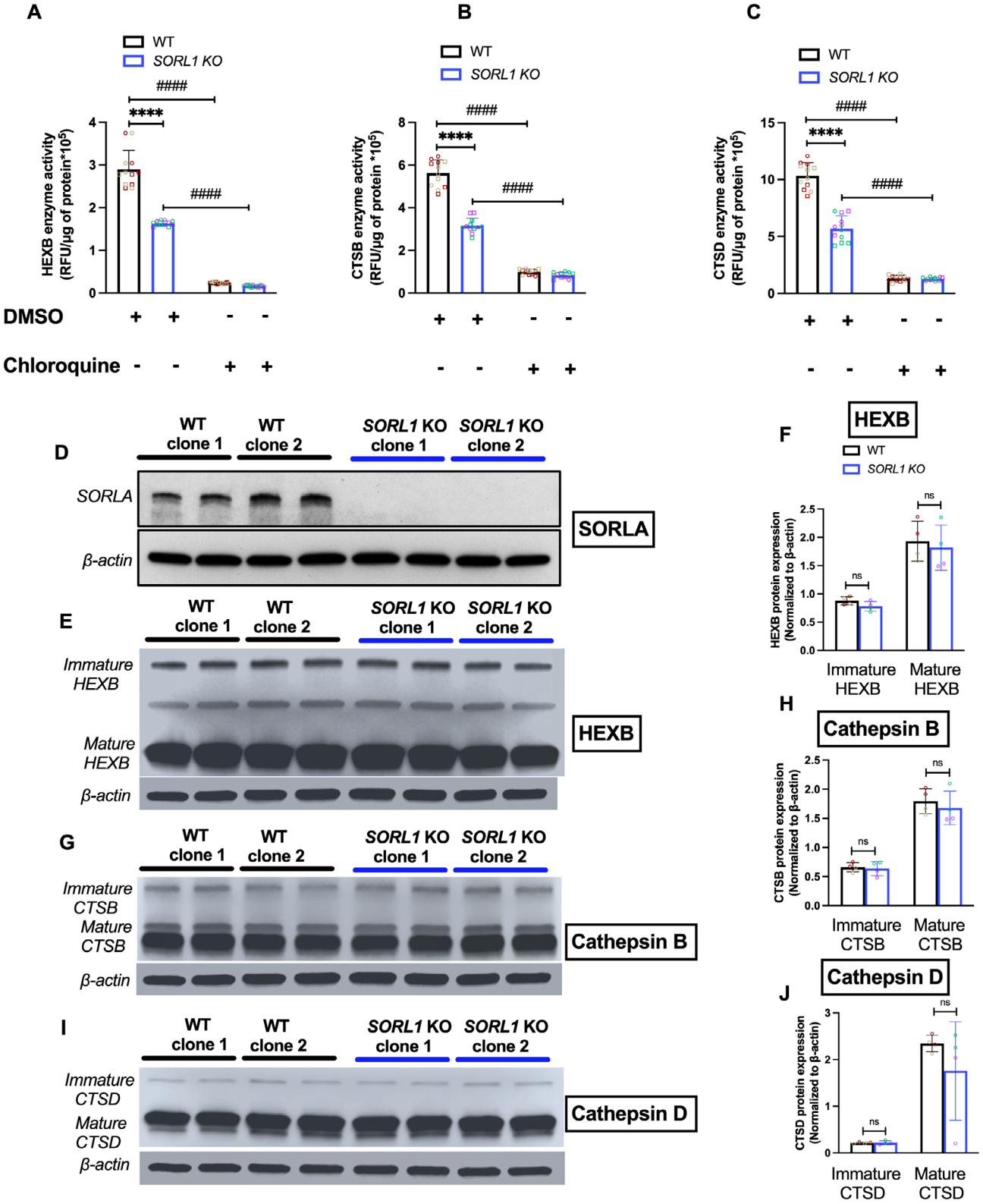

FIGURE 2 | Legend on next page.

FIGURE 2 | Loss of *SORL1* results in decreased lysosomal enzyme activity in hMGLs. (A–C) Enzyme activity assays based on fluorometric detection show reduced enzyme activity of lysosomal enzymes (A) HEXB, (B) Cathepsin B, and (C) Cathepsin D in *SORL1* KO hMGLs as compared to WT hMGLs. Both WT and *SORL1* KO hMGLs show reduced enzyme activity of all the enzymes tested when treated with the lysosome function inhibitor, chloroquine, which was used as a control. (D–I) Western blotting demonstrates loss of SORLA protein expression (D) but no change in total protein levels of immature and mature forms of HEXB (E-F), Cathepsin B (G and H) and Cathepsin D (I and J) in *SORL1* KO hMGLs relative to WT hMGLs. For the enzyme activity assays, two isogenic clones per genotype (WT and *SORL1* KO) and six independent replicates (two differentiations and three-technical replicates per differentiation) per clone per genotype ($N = 12$ independent replicates) were used, and for the western blot experiments, two isogenic clones per genotype (WT and *SORL1* KO) and two independent replicates (one differentiation and two technical replicates) per clone per genotype ($N = 4$ independent replicates) were utilized. Data are represented as mean ± SD and analyzed using a parametric two-tailed unpaired t test and two-way ANOVA with Tukeys multiple comparison test. Significance while comparing WT to *SORL1* KO hMGLs was defined and depicted as a value of $^{*}p < 0.05$, $^{**}p < 0.01$, $^{***}p < 0.001$, and $^{****}p < 0.0001$, ns = not significant, and while comparing different treatments of each genotype was defined and depicted as a value of $\#p < 0.05$, $\#\#p < 0.01$, $\#\#\#p < 0.001$, and $\#\#\#\#p < 0.0001$, ns = not significant.

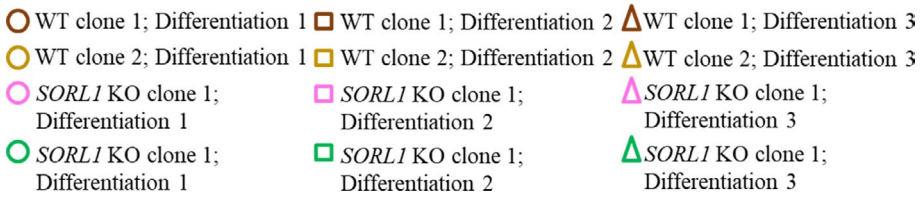

retromer complex (Fjorback et al. 2012) for various sorting functions, and the retromer complex associates with CIMPR to regulate the sorting of lysosomal enzymes (Cui et al. 2019; Nielsen et al. 2007). Thus, we hypothesized that the loss of SORLA would result in altered trafficking of lysosomal enzymes from the TGN to the lysosomes. To test whether lysosomal enzymes are intracellularly mislocalized with the loss of *SORL1*, we used immunocytochemistry with antibodies that recognized both immature and mature forms of the lysosomal enzymes Cathepsin B, Cathepsin D, and HEXB. We measured colocalization of these enzymes at the TGN and late endosomes and lysosomes using the TGN marker TGN38 and the late endosome and lysosome marker LAMP1. Our results showed increased colocalization of all three enzymes with TGN38 (Figure 3A,C,E) and decreased colocalization with LAMP1 (Figure 3B,D,F) suggesting that the enzymes are not appropriately trafficked to lysosomes from the TGN. As we observed decreased enzyme activity but no change in total protein expression of CTSD, CTSB, and HEXB, our data suggested that dysfunction in lysosomal degradation is likely due to mistrafficking of lysosomal enzymes.

3.4 | Loss of *SORL1* Results in Reduced Protein Levels and Dysfunctional Trafficking of CIMPR From the TGN to the Lysosomes in hMGLs

To further investigate the mechanism that causes dysfunctional trafficking of lysosomal enzymes in *SORL1* KO hMGLs, we tested if the loss of SORLA causes altered expression and/or intracellular localization of the lysosomal enzyme trafficking protein, CIMPR. We measured colocalization of CIMPR at the TGN, using the TGN marker TGN38, and at late endosomes and lysosomes using LAMP1. Our data showed that *SORL1* KO hMGLs had reduced colocalization of CIMPR with LAMP1 and no change in colocalization with TGN38 (Figure 4A,B), suggesting that the loss of *SORL1* leads to an impaired CIMPR-dependent trafficking pathway of lysosomal enzymes out of the TGN to lysosomes. Additionally, we observed reduced protein levels of CIMPR in *SORL1* KO hMGLs as compared to WT hMGLs by Western blot analysis (Figure 4C–D). Overall, these data demonstrate that depletion of SORLA results in altered protein expression and intracellular localization of the trafficking protein CIMPR, contributing to dysfunctional trafficking of lysosomal enzymes observed in *SORL1* KO hMGLs.

3.5 | Loss of *SORL1* Causes Lysosomal Accumulation of Aβ and Synaptosomes in hMGLs

Given that depletion of *SORL1* causes reduced lysosomal degradation in hMGLs, we next hypothesized that phagocytosed substrates might accumulate in lysosomes in *SORL1*-deficient hMGLs. To test this idea, we measured lysosomal accumulation of fluorophore-labeled fibrillar Aβ 1–42 (fAβ) and CM-Dil dye-labeled synaptosomes using pulse-chase assays and immunocytochemistry. Consistent with our hypothesis, *SORL1* KO hMGLs showed increased accumulation of both substrates as evidenced by increased colocalization of Aβ 1–42 (Figure 5A,B) and synaptosomes (Figure 5C,D) with LAMP1. To further confirm that reduced lysosomal catabolism contributes to intracellular accumulation of both substrates, lysosomal catabolism was inhibited by chloroquine, and lysosomal accumulation of fAβ and synaptosomes was measured. As expected, chloroquine treatment caused a significant increase in lysosomal accumulation of both substrates in both WT and *SORL1* KO hMGLs (Figure 5B,D). Increased phagocytosis can contribute to increased accumulation of these substrates, so we tested whether phagocytic uptake was altered in *SORL1* KO hMGLs. To analyze uptake and phagocytosis, we incubated cells with fluorophore-labeled fAβ and synaptosomes for 30 min, 5 h, and 24 h and observed increased uptake and sustained phagocytosis of both substrates in *SORL1* KO hMGLs as compared to WT hMGLs (Figure S4D–G). Interestingly, we did not observe a difference in internalization of oligomeric Aβ (Figure S4C), consistent with previous reports (Ovesen et al. 2024). This suggests that *SORL1* may alter phagocytic uptake in a substrate-specific manner or that the dynamics of this process may be variable. Because we consistently observed increased uptake of fAβ and synaptosomes, we

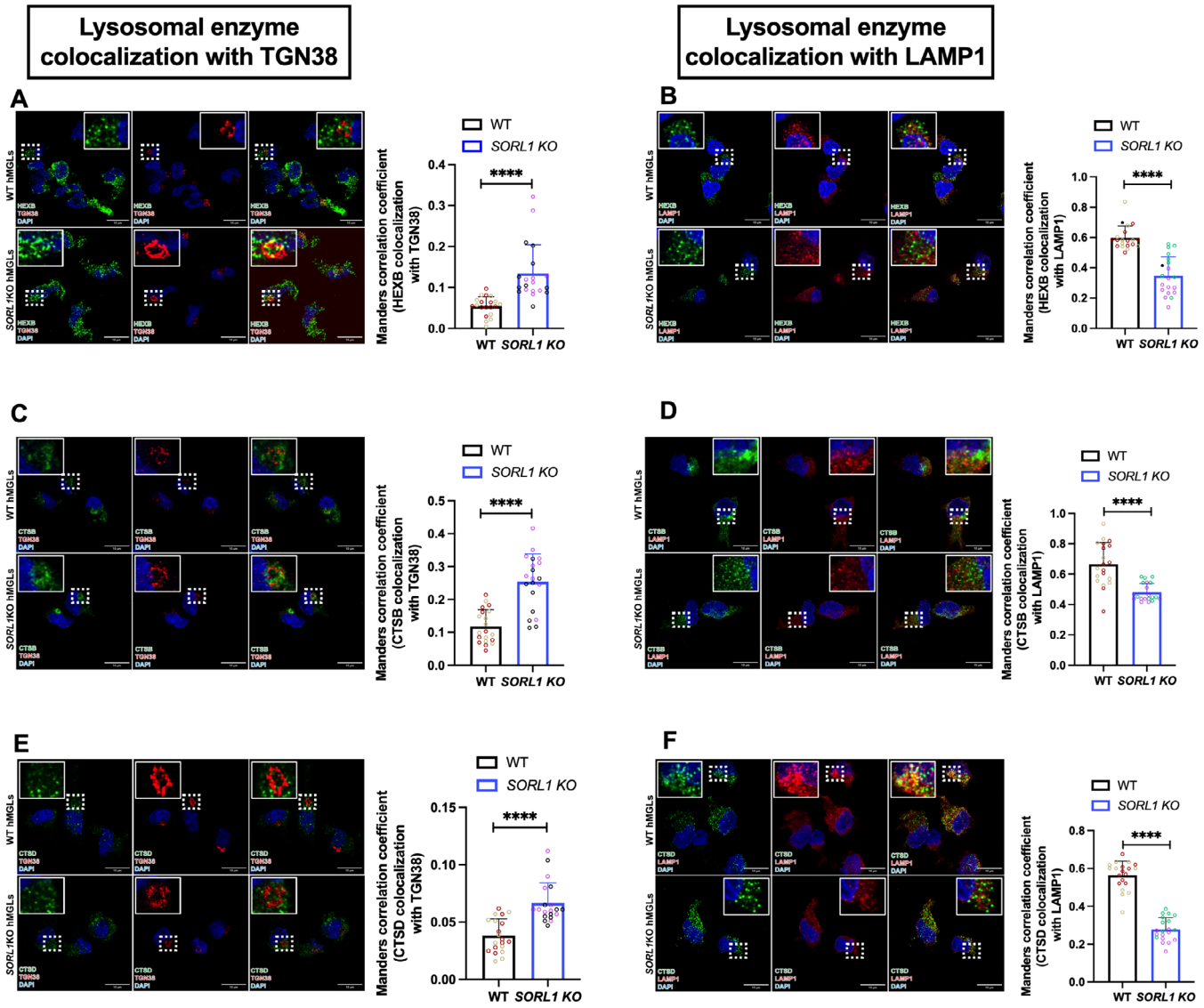

FIGURE 3 | Loss of *SORL1* results in altered trafficking of lysosomal enzymes in hMGLs Immunocytochemistry and colocalization analysis were used to measure the colocalization of lysosomal enzymes HEXB, Cathepsin B, and Cathepsin D with TGN and lysosomes using TGN38 and LAMP1 antibodies, respectively. As compared to WT hMGLs, *SORL1* KO hMGLs show increased colocalization of all the enzymes with TGN38 (A,C,E) and decreased colocalization of all enzymes with LAMP1 (B,D,F) suggestive of altered trafficking of lysosomal enzymes from TGN to lysosomes. Colocalization was measured using the JACOP plugin in Image J software and presented as Manders correlation coefficient. Scale bar = 10 μm. Two isogenic clones per genotype (WT and *SORL1* KO) and 10 images per clone per genotype ($N = 20$ independent replicates) were used for these experiments. Each image comprised at least 5–10 cells, and hence a total of 50–100 cells per clone per genotype were analyzed for colocalization analysis. Data represented as mean ± SD and analyzed using a parametric two-tailed unpaired *t* test. Significance while comparing WT to *SORL1* KO hMGLs was defined and depicted as a value of $*p < 0.05$, $**p < 0.01$, $***p < 0.001$, and $****p < 0.0001$; ns = not significant.

WT clone 1; Differentiation 1 | WT clone 1; Differentiation 2 | WT clone 1; Differentiation 3
WT clone 2; Differentiation 1 | WT clone 2; Differentiation 2 | WT clone 2; Differentiation 3
SORL1 KO clone 1; Differentiation 1 | *SORL1* KO clone 1; Differentiation 2 | *SORL1* KO clone 1; Differentiation 3
SORL1 KO clone 1; Differentiation 1 | *SORL1* KO clone 1; Differentiation 2 | *SORL1* KO clone 1; Differentiation 3

wondered whether loss of SORLA expression might alter cell surface localization of phagocytic receptors. To test this idea, we analyzed cell surface localization of two key phagocytic receptors known to be involved in phagocytosis of fibrillar Aβ and synaptosomes. TREM2 is known to phagocytose fibrillar Aβ and synaptosomes in microglia (La Rosa et al. 2023; McQuade et al. 2020) and the P2Y6 receptor is a potent phagocytic receptor involved in microglial phagocytosis of synaptosomes (Dundee and Brown 2024; Dundee et al. 2023). We observed increased surface localization of both receptors in *SORL1* KO hMGLs (Figure S5A–D) without alteration of total protein levels of TREM2 and P2Y6 receptor (Figure S5E–F) suggesting that

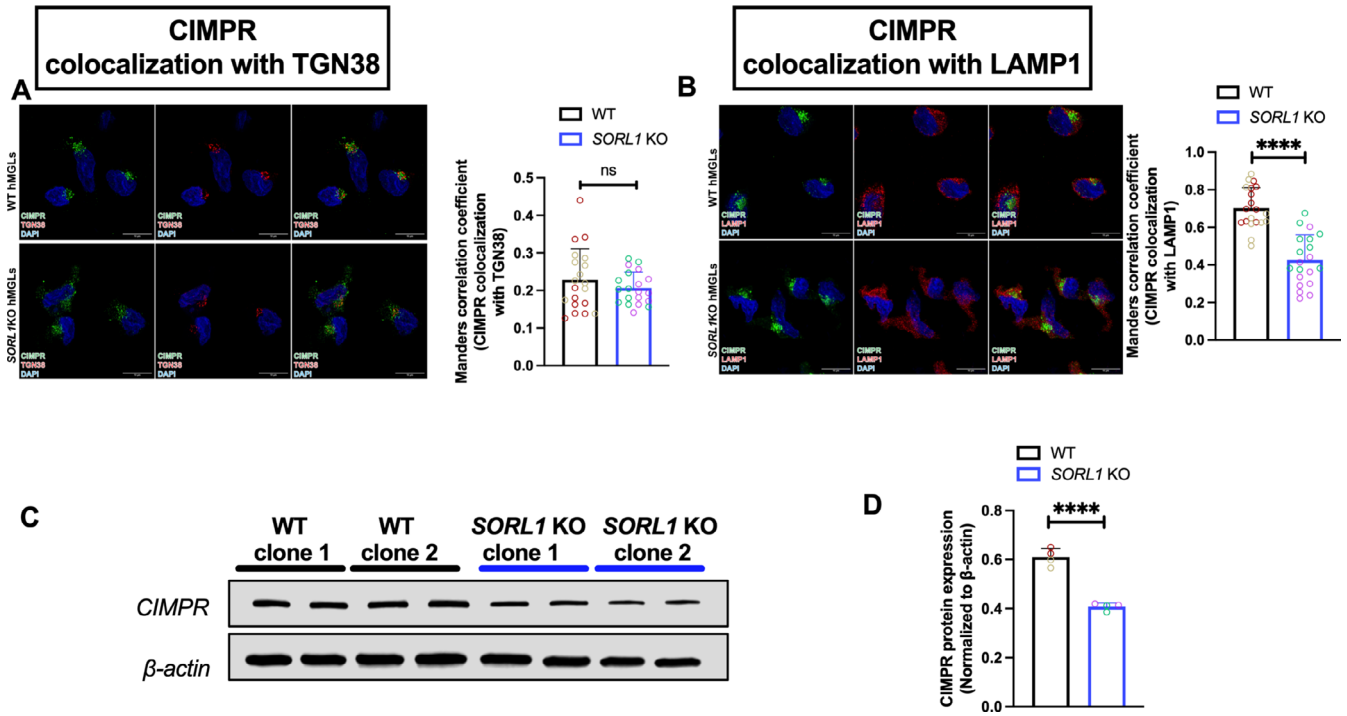

FIGURE 4 | Loss of *SORL1* results in reduced protein levels and dysfunctional trafficking of Cation-independent Mannose-6-phosphate receptor (CIMPR), from the TGN to the lysosomes in hMGLs (A and B) Immunocytochemistry and colocalization analysis were used to measure colocalization of CIMPR with TGN and late endosomes and lysosomes using TGN38 and LAMP1 antibodies, respectively. As compared to WT hMGLs, *SORL1* KO hMGLs show no change in colocalization of CIMPR with TGN38 (A) and decreased colocalization of CIMPR with LAMP1 (B). (C and D) Western blot and quantification showing decreased protein levels of CIMPR in *SORL1* KO hMGLs as compared to WT hMGLs. Colocalization was measured using JACOP plugin in Image J software and presented as Manders correlation coefficient. Scale bar = 10 μm. 2 isogenic clones per genotype (WT and *SORL1* KO) and 10 images per clone per genotype ($N = 20$ independent replicates; 1 differentiation) were used for these experiments. Each image comprised at least 5–10 cells, and hence a total of 50–100 cells per clone per genotype were analyzed for colocalization analysis. Data represented as mean ± SD and analyzed using a parametric two-tailed unpaired t test. Significance while comparing WT to *SORL1* KO hMGLs was defined and depicted as a value of $^{*}p < 0.05$, $^{**}p < 0.01$, $^{***}p < 0.001$, and $^{****}p < 0.0001$; ns = not significant.

WT clone 1; Differentiation 1 | WT clone 1; Differentiation 2 | WT clone 1; Differentiation 3
WT clone 2; Differentiation 1 | WT clone 2; Differentiation 2 | WT clone 2; Differentiation 3
SORL1 KO clone 1; Differentiation 1 | *SORL1* KO clone 1; Differentiation 2 | *SORL1* KO clone 1; Differentiation 3
SORL1 KO clone 1; Differentiation 1 | *SORL1* KO clone 1; Differentiation 2 | *SORL1* KO clone 1; Differentiation 3

SORLA may play a role in maintaining the number of receptors at the cell surface required for phagocytosis, and its absence causes aberrant localization of these receptors. We also tested uptake of a general endocytosis marker, transferrin conjugated to Alexa fluor 647, and also showed increased uptake of this substrate in *SORL1* KO hMGLs (Figure S4B). Overall, these data suggest that, in our hMGLs, SORLA may increase phagocytosis of fibrillar Aβ and synaptosomes by increasing surface localization of phagocytic receptors, TREM2 and P2Y6, in hMGLs. Together, our data demonstrate that through increased phagocytic uptake combined with impaired lysosomal degradation, loss of *SORL1* significantly increases lysosomal dysfunction in human microglia.

3.6 | Loss of *SORL1* Decreases LE in hMGLs

Accumulation of substrates in lysosomes with impaired degradative capacity can add to further lysosomal stress. LE is an alternate pathway to release lysosomes and their contents from cells (Wang, Gómez-Sintes, et al. 2018; Zhong et al. 2023). LE is a calcium-dependent process that involves fusion of lysosomes with the plasma membrane, exposing the luminal domain of LAMP1 on the cell surface, resulting in release of lysosomal contents into the extracellular environment (Andrews 2000; Blott and Griffiths 2002). Immune cells use LE to remodel the extracellular environment and to release some pro-inflammatory cytokines (Buratta et al. 2020; Tancini et al. 2020). Murine microglia are known to utilize LE to maintain cellular homeostasis and respond to external stimuli by releasing lysosomal enzymes and cytokines outside the cell (Andrei et al. 2004; Dou et al. 2012; Eder 2009). We tested whether the process of LE might be altered because of lysosome dysfunction observed in *SORL1* KO hMGLs. We induced LE with the ionophore calcimycin (Jaiswal et al. 2002) and labeled cells with an antibody specific to the luminal epitope of LAMP1 (Andrews 2017) to visualize cell surface localization of LAMP1 via flow cytometry and immunocytochemistry.

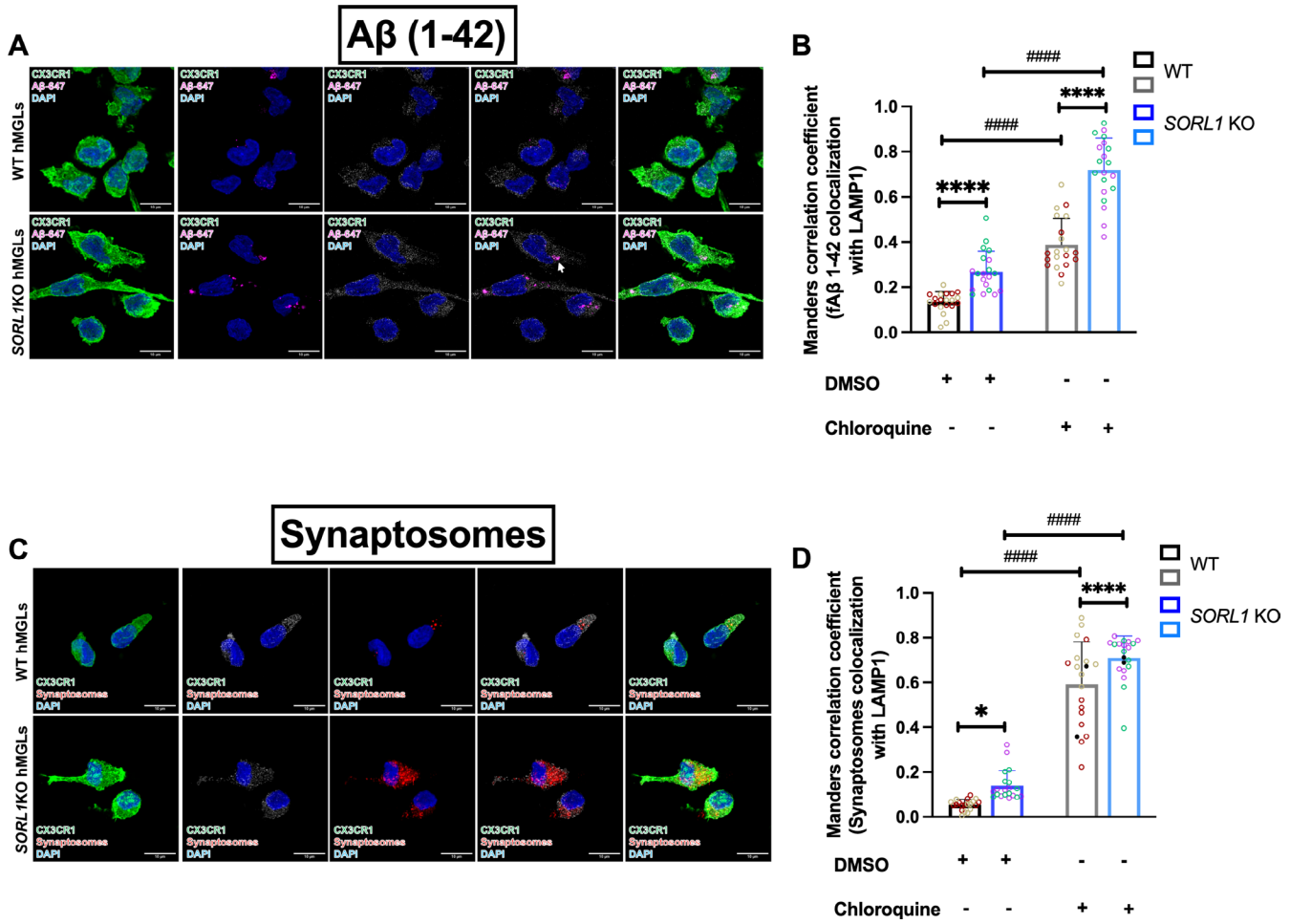

FIGURE 5 | Loss of *SORL1* causes increased lysosomal accumulation of fibrillar Aβ 1–42 (fAβ) and synaptosomes in hMGLs (A–D) Immunocytochemistry and colocalization analysis with and without treatment with chloroquine show increased colocalization of fAβ (A and B) and synaptosomes (C and D) with the lysosome marker, LAMP1, in *SORL1* KO hMGLs as compared to WT hMGLs, suggestive of increased lysosomal accumulation. Chloroquine-treated WT and *SORL1* KO hMGLs show increased lysosomal accumulation of both substrates as compared to their untreated counterparts. Colocalization analysis was performed using the JACOP plugin of Image J software, and data is presented as the Manders correlation coefficient. Scale bar = 10 μm. Two isogenic clones per genotype (WT and *SORL1* KO) and 10 images per clone per genotype ($N = 20$ independent replicates; 1 differentiation) were used for these experiments. Each image comprised at least 5–10 cells, and hence a total of 50–100 cells per clone per genotype were analyzed for colocalization analysis. Data are represented as mean ± SD and analyzed using a parametric two-tailed unpaired t test and two-way ANOVA with Tukeys multiple comparison test. Significance while comparing WT to *SORL1* KO hMGLs was defined and depicted as a value of $*p < 0.05$, $**p < 0.01$, $***p < 0.001$, and $****p < 0.0001$, ns = not significant, and while comparing different treatments of each genotype was defined and depicted as a value of $\#p < 0.05$, $\#\#p < 0.01$, $\#\#\#p < 0.001$, and $\#\#\#\#p < 0.0001$, ns = not significant.

WT clone 1; Differentiation 1
WT clone 1; Differentiation 2
WT clone 1; Differentiation 3
WT clone 2; Differentiation 1
WT clone 2; Differentiation 2
WT clone 2; Differentiation 3
SORL1 KO clone 1; Differentiation 1
SORL1 KO clone 1; Differentiation 2
SORL1 KO clone 1; Differentiation 3
SORL1 KO clone 1; Differentiation 1
SORL1 KO clone 1; Differentiation 2
SORL1 KO clone 1; Differentiation 3

Measurement of surface LAMP1 localization has been repeatedly used as a robust readout of LE (Haka et al. 2016; Lee et al. 2024; Verma et al. 2023; Zhong et al. 2023). Both WT and *SORL1* KO hMGLs showed an increase in cell-surface localization of LAMP1 upon calcimycin treatment, suggesting that hMGLs can undergo LE in vitro. However, *SORL1* KO hMGLs exhibited reduced surface LAMP1 localization as compared to WT in both stimulated and unstimulated conditions, as evidenced by immunocytochemistry (Figure 6A) and flow cytometry (Figure 6B) showing that loss of *SORL1* results in decreased LE in hMGLs. This decrease was not due to the reduced total protein expression of LAMP1 (Figure 6C). Because LE causes extracellular release of lysosomal enzymes, we measured extracellular lysosomal enzyme activity and total levels of extracellular lysosomal enzymes. We found reduced extracellular enzyme activity of HEXB, Cathepsin B, and Cathepsin D (Figure 6D–F) and reduced protein levels of all three lysosomal enzymes in cell culture media (Figure S3A–D) in *SORL1* KO hMGLs upon treatment with a LE activator, calcimycin. While the reduction in extracellular enzyme activity

and protein is likely due to the altered trafficking of hydrolases, taken together along with the reduction in cell surface LAMP1 localization, this strongly indicates that important components of LE are impaired in *SORL1* KO hMGLs. Because the extracellular release of lysosomal enzymes is a normal part of LE, often contributing to extracellular matrix remodeling, cell–cell communication (Buratta et al. 2020) and ability to digest large extracellular substrates (Haka et al. 2016) the general reduction in lysosomal enzyme activity observed in *SORL1* hMGLs may further confound the LE process. To further confirm our hypothesis, we used fluorometric detection to measure extracellular lysosomal enzyme activity of HEXB and Cathepsin D as a readout of LE in a second model of hMGLs (Dolan et al. 2023). *SORL1* KO hMGLs showed decreased extracellular enzyme activity of both enzymes (Figure S2C,D), validating the idea that loss of *SORL1* impairs LE in hMGLs irrespective of the method used to generate microglia from hiPSCs. To test whether LE contributes to secretion of cytokines and to assess the contribution of SORLA to this process, we first assessed levels of a cytokine known to be released by LE in immune cells, IL-1β (Andrei et al. 2004; Gardella et al. 2001; Monif et al. 2016) and a cytokine known to be modulated by SORLA, IL-6 (Larsen and Petersen 2017), with and without treatment with the LE activator, calcimycin. We measured both extracellular and intracellular levels of both cytokines upon treatment with DMSO, calcimycin, and pro-inflammatory stimuli, LPS, and IFN-γ. Our data showed a significant increase in extracellular secretion and no change in intracellular protein expression of both cytokines upon treatment with calcimycin (Figure 6G,J; Figure S6A,D). These data suggest that calcimycin increases secretion of cytokines by increasing LE rather than by activating microglia. Interestingly, we saw a slight decrease in the levels of IL-6 released after calcimycin treatment in *SORL1* KO hMGLs (Figure 6F), suggesting that altered levels of LE in these cells may affect release of this cytokine. Calcimycin-related secretion of IL1-β levels was unaffected in *SORL1* KO hMGLs, although intracellular protein levels of IL1-β were reduced (Figure S6).

3.7 | Loss of *SORL1* Results in Overall Decreased Inflammatory Response in hMGLs

While we noticed a slight but significant blunting of IL-6 in response to calcimycin treatment, we also observed a larger decrease in the secretion and expression of IL-6 in response to canonical stimuli, LPS and IFNγ (Figure 6H,I,K,L). A recent study demonstrated that SORLA has a key role in the sorting of the pattern recognition receptor CD14 (Ovesen et al. 2024) Similar to their findings, we also observed a blunted response of multiple pro-and anti-inflammatory cytokines to LPS treatment, and we also show a blunted response to IFNγ stimulation. Specifically, *SORL1* KO hMGLs showed decreased extracellular secretion of pro-inflammatory cytokines IL-1β, IL-15, IP-10, TNF-α, and IL-8 and anti-inflammatory cytokines IL-10, IL-13, and IL-2 (Figures S6 and S7). As aberrant lysosome function can negatively impact the neuroimmune response of microglia (Quick et al. 2023; Van Acker et al. 2021), our data, along with that of Ovesen et al., suggests that there are several mechanisms by which SORLA-related trafficking can affect pro-inflammatory responses that are important in AD.

4 | Discussion

Despite extensive evidence that loss-of-function variants in the *SORL1* gene and *SORL1* haploinsufficiency are causative for AD (Campion et al. 2019; Holstege et al. 2017; Nicolas et al. 2016; Pottier et al. 2012; Verheijen et al. 2016), developing therapeutic interventions targeting *SORL1* has been challenging, partly because cell-type-specific mechanisms through which loss of *SORL1* may increase risk for AD remain unclear. Indeed, recent RNA sequencing data highlight that certain CNS cells undergo more changes than others in response to *SORL1* KO (Lee et al. 2023). Recent work from our group and others has shown that depletion of SORLA in neurons leads to enlarged early endosomes, impairments in endo-lysosomal trafficking, changes in gene expression, and impaired neuronal function (Hung et al. 2021; Knupp et al. 2020; Lee et al. 2023; Mishra et al. 2023, 2022). Despite this extensive characterization in neurons, very little is currently understood about SORLA function in human microglia. Our previous work suggests that there may be important cell-type-specific differences in endo-lysosomal organelles affected by loss of SORLA. We did not observe differences in the size of early endosomes between *SORL1* WT and *SORL1* KO hMGLs (Knupp et al. 2020) but have documented lysosomal enlargement in *SORL1* KO microglia (Mishra 2024). Here we provide evidence for the role of SORLA in regulating lysosome function in human microglia. We show that loss of SORLA causes mistrafficking of lysosomal enzymes, leading to impaired lysosomal degradation and accumulation of substrates in lysosomes. Alternate pathways to release lysosomal cargo from cells, such as LE, are also impaired. This impairment contributes to a blunted neuroimmune response.

SORLA binds to retromer (Fjorback et al. 2012), which regulates the retrograde transport of the cation-independent mannose-6-phosphate receptor (CIMPR) through the mannose-6-phosphate-dependent pathway (M6P) (Arighi et al. 2004; Cui et al. 2019). The CIMPR is a key receptor that traffics lysosomal enzymes from the TGN to the lysosomes (Braulke and Bonifacino 2009; Braulke et al. 2023). In the absence of SORLA, there is reduced expression and reduced localization of CIMPR in late endosomes and lysosomes, suggesting that this crucial pathway for the delivery of lysosomal hydrolases is impaired in *SORL1* KO hMGLs. During the process of lysosomal enzyme trafficking to the late endosomes and lysosomes, CIMPR forms a complex with premature lysosomal enzymes at the TGN, is transported to the early endosomes, and then directed towards the lysosomes (Hasanagic et al. 2015). Given that we do not see any difference in the localization of this receptor at the TGN but reduced localization at the late endosomes and lysosomes, it is conceivable that CIMPR gets stuck in the early endosomes during lysosomal enzyme trafficking in the absence of SORLA. In support of this idea, it has been shown in immortalized neuroblastoma and epithelial cell lines that SORLA can bind to the cytosolic adaptor protein, phosphofurin acidic cluster sorting protein 1 (PACS1) (Burgert et al. 2013) which is known to direct retrograde TGN retrieval of CIMPR (Chen et al. 1997; Scott et al. 2006; Wan et al. 1998) and can participate in PACS1-dependent sorting of Cathepsin B (Burgert et al. 2013; Nielsen et al. 2007). However, whether SORLA directly binds to CIMPR and the precise role of SORLA in the M6P-dependent pathway in microglia warrants further investigation.

We did not observe significant differences in total protein or changes in pro versus mature forms of lysosomal enzymes (Figure 2D–F). One explanation for this observation could be that there are different ratios of pro versus mature forms of these enzymes in other compartments (such as endosomes) or that there is leakage of mature enzymes from the lysosome to the cytoplasm. Interestingly, proteomic analyses have variability in the expression of lysosomal enzymes from *SORL1*-deficient microglia, in one case showing no change (Lee et al. 2023) and in another showing decreased expression, although the majority of this decrease was reported from a cell line with a missense variant in the VPS10 domain of *SORL1* (Liu et al. 2020).

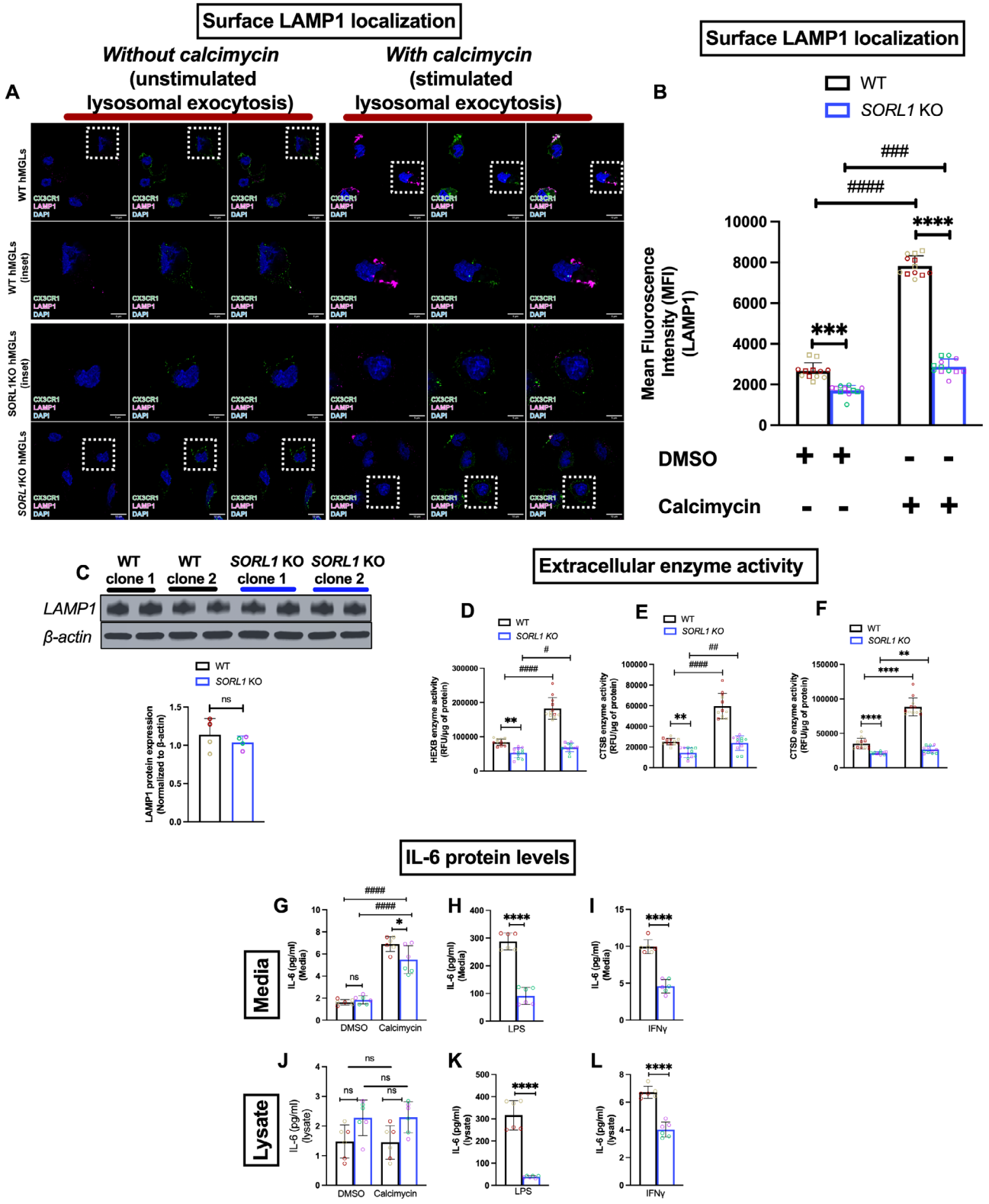

FIGURE 6 | Legend on next page.

FIGURE 6 | Loss of *SORL1* causes reduced lysosomal exocytosis in hMGLs (A and B). Surface localization of LAMP1 measured by immunocytochemistry and flow cytometry as a readout of LE (A) Immunocytochemistry with antibody specific for the N terminal luminal epitope of LAMP1 and microglia marker, CX3CR1 demonstrating decreased surface localization of LAMP1 in *SORL1* KO hMGLs as compared to WT hMGLs. (B) Quantification by flow cytometry showing decreased MFI of LAMP1 antibody in *SORL1* KO hMGLs relative to WT hMGLs suggestive of decreased LE with loss of *SORL1* in hMGLs. (C) Western blot and quantification shows no change in protein expression of LAMP1 in *SORL1*KO hMGLs relative to WT hMGLs. (D–F) Extracellular enzyme activity of lysosomal enzymes measured as a readout of LE. Enzyme activity assays demonstrate decreased lysosomal enzyme activity of (D) HEXB, (E) Cathepsin B, and (F) Cathepsin D in *SORL1* KO hMGLs as compared to WT hMGLs suggestive of decreased LE with loss of *SORL1* in hMGLs. (G–L) Cytokine secretion of IL-6 measured by ELISA shows increased extracellular secretion of IL-6 upon calcimycin treatment in both WT and *SORL1* KO hMGLs without increase in intracellular protein expression but *SORL1* KO hMGLs show decreased secretion of IL-6 in response to calcimycin as compared to WT hMGLs (G, J). *SORL1* KO hMGLs show reduced extracellular secretion and intracellular protein levels of IL-6 in response to pro-inflammatory stimuli LPS and IFNγ relative to WT hMGLs (H, I, K, L). Two isogenic clones per genotype (WT and *SORL1* KO) and 6 independent replicates (two differentiations and three technical replicates) per clone per genotype ($N = 12$ independent replicates) were used for these experiments. Data represented as mean ± SD and analyzed using parametric two-tailed unpaired t test and 2-way ANOVA with Tukeys multiple comparison test. Significance while comparing WT to *SORL1* KO hMGLs was defined and depicted as a value of $*p < 0.05$, $**p < 0.01$, $***p < 0.001$, and $****p < 0.0001$, ns = not significant and while comparing different treatments of each genotype was defined and depicted as a value of $\#p < 0.05$, $\#\#p < 0.01$, $\#\#\#p < 0.001$, and $\#\#\#\#p < 0.0001$, ns = not significant.

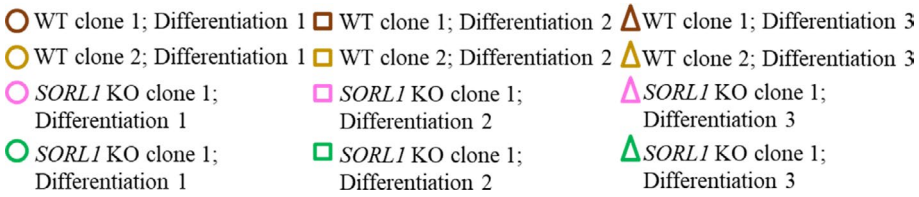

Impaired degradation in SORLA deficient hMGLs affects the fate of phagocytosed substrates. We observed increased internalization of various substrates including transferrin, fAβ, and synaptosomes (Figure S5). Interestingly, we did not see a change in phagocytosis of oAβ, which replicates recently published work (Ovesen et al. 2024). The impact of increased phagocytosis of synaptosomes could contribute to excessive synaptic pruning and eventual synaptic loss observed in AD, but increased uptake of fAβ may be a means to reduce amyloidogenic burden. SORLA is known to regulate receptor protein homoeostasis at the cell surface by modulating intracellular sorting of receptors to the TGN and endo-lysosomal compartments (Pietilä et al. 2019; Schmidt et al. 2017). We observed increased cell surface localization of the phagocytic receptors P2Y6 and TREM2 (Figure S5) which may explain the increased internalization of certain substrates. Another recent study observed increased expression of the AD risk gene *BIN1* in *SORL1* KO hMGLs (Lee et al. 2023), which may also lead to increased phagocytosis (Sudwarts et al. 2022). Liu et al. observed expression changes in phagocytic receptors in *SORL1* deficient hMGLs including *TREM2* and *ITGB2*, a receptor involved in the phagocytosis of both Aβ and synaptosomes (Liu et al. 2020). However, in their study, Liu et al. observed deficient phagocytosis of oligomeric Aβ, although the assay did not distinguish between phagocytic uptake and substrate degradation. Mechanisms of phagocytic uptake by microglia can also differ significantly depending on the protein conformation of Aβ (Lee et al. 2023; Pan et al. 2011; Ries and Sastre 2016; Sudwarts et al. 2022). Together, this data suggests that loss of *SORL1* expression may change localization of phagocytic receptors and genes involved in phagocytosis of specific substrates.

While we observe increased phagocytic uptake of both fAβ and synaptosomes, these substrates were not degraded; therefore, a crucial aspect of the normal phagocytic process in *SORL1* KO hMGLs is impaired, leading to their intracellular accumulation. This may ultimately increase lysosomal stress in microglia and contribute to lysosomal dysfunction seen in AD. Indeed, the role of SORLA in microglial phagocytosis may act as a "double-edged sword," functioning in both a disease-stage-specific and context-dependent manner.

LE is used by microglia to release cytokines, enzymes, and cargo into the extracellular space (Dou et al. 2012; Jacquet et al. 2024; Kreher et al. 2021). LE is a calcium-regulated process that expels lysosomal contents into the extracellular space (Buratta et al. 2020; Tancini et al. 2020). LE is important for such activities as remodeling of the extracellular matrix and, in the case of immune cells, releasing contents to degrade pathogenic material (Ireton et al. 2018; Miao et al. 2015). We found that *SORL1* KO hMGLs show reduced LE as evidenced by reduced LAMP1 localization on the plasma membrane and reduced enzyme activity in the conditioned medium of hMGLs after treatment with a stimulus. Thus, the increased accumulation of substrates in lysosomes may also indicate a failure to release these substrates via LE.

Interestingly, in response to acute stress, LE can be used to release pro-inflammatory cytokines, bypassing the slower, more conventional secretory pathway (Aiello et al. 2020). We observed that calcimycin-induced LE can release IL-1β and IL-6, with the IL-6 response being reduced in *SORL1* KO hMGLs. We also observed a blunted cytokine release in response to canonical pro-inflammatory stimuli, LPS, and IFNγ, consistent with other recent reports in SORLA-deficient hMGLs (Ovesen et al. 2024), suggesting that multiple mechanisms may govern SORLA-mediated cytokine release in hMGLs.

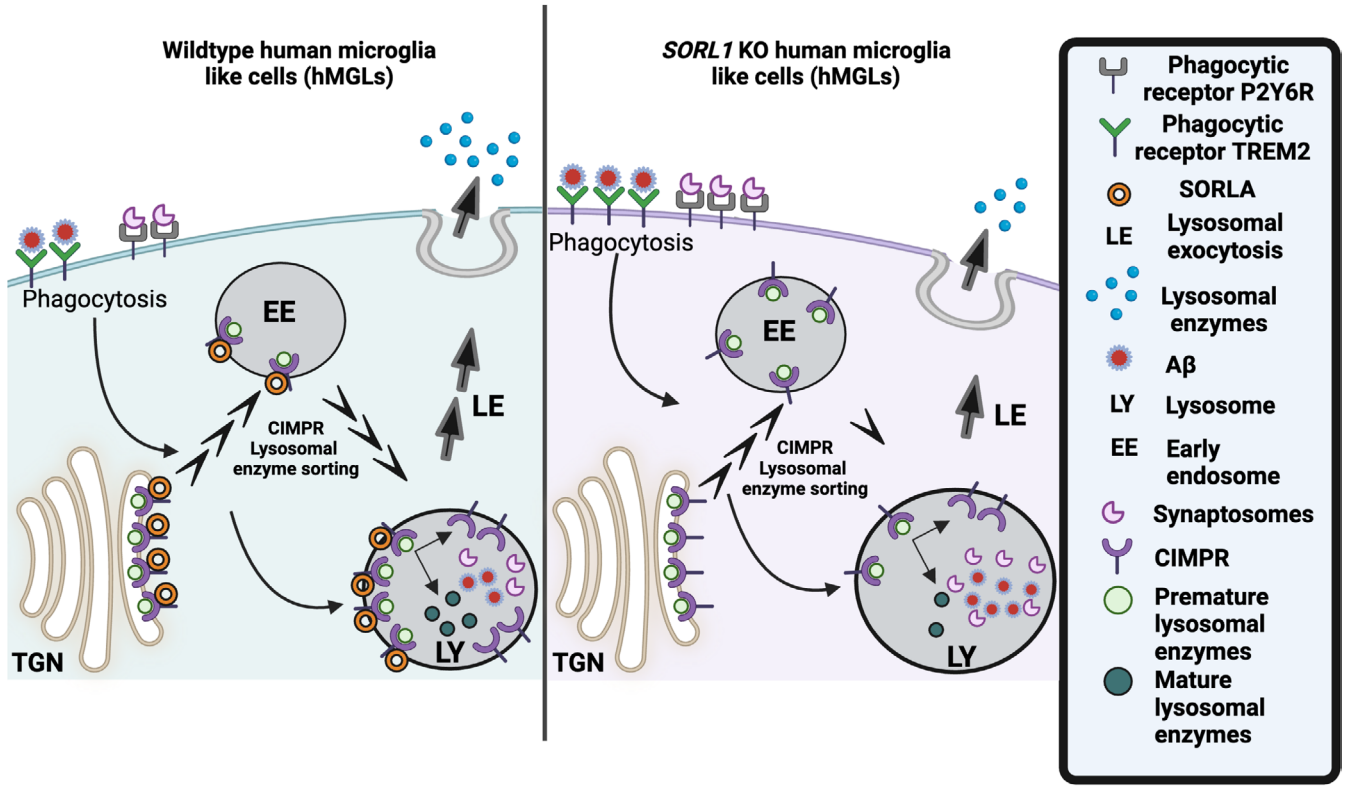

FIGURE 7 | Working model. We propose the following working model that underpins the abnormal lysosomal phenotypes observed in *SORL1* KO hMGLs. Loss of *SORL1* (orange circle) leads to decreased lysosomal degradation and decreased lysosomal enzyme activity caused by impaired trafficking of CIMPR and lysosomal enzymes from the TGN. Loss of *SORL1* also causes enhanced phagocytic uptake due to increased cell surface localization of phagocytic receptors, but due to the decreased degradative capacity of the lysosomes, there is lysosomal accumulation of substrates including fibrillar Aβ 1–42 and synaptosomes. Alternate pathways of lysosomal clearance such as lysosomal exocytosis are also impaired, contributing to a blunted neuroimmune response. Altogether, loss of *SORL1* causes increased lysosomal stress in human microglia.

4.1 | Working Model

Altogether, we propose a working model that underpins the abnormal lysosomal phenotypes observed in *SORL1* KO hMGLs (Figure 7). Loss of *SORL1* impairs the trafficking of lysosomal enzymes from the TGN to the lysosome via the M6P pathway, leading to inefficient degradation of phagocytosed substrates that accumulate in lysosomes. Alternate pathways of lysosomal clearance, such as LE, are also impaired. Furthermore, the depletion of *SORL1* may decrease the release of pro-inflammatory cytokines either through conventional secretory routes from the TGN to the cell surface or by impairing LE, as observed in our study and others (Ovesen et al. 2024). In the context of AD, we posit that lysosome dysfunction in microglia caused by the loss of *SORL1* may result in heightened lysosomal stress caused by increased accumulation of substrates and a stunted inflammatory response to accumulating pathogenic proteins in the extracellular brain environment. Since the loss of *SORL1* is observed in the early stages of AD, hypofunctional microglia with depleted SORLA may initially contribute to AD pathogenesis through lysosome dysfunction.

5 | Conclusions

In summary, our study highlights lysosome dysfunction in microglia as a pathway through which *SORL1* loss of function may increase the risk for AD. Our data identify a previously unexplored cell-type-specific mechanism through which *SORL1* can regulate the endo-lysosomal pathway beyond its well-established function as a sorting receptor for APP in neurons, illustrating the importance of exploring this multifaceted sorting receptor and potent AD risk factor as a therapeutic target for AD.

6 | Limitations of the Study

We recognize our study has several limitations. In vitro studies using hiPSC-derived microglia do not allow thorough representation of cellular complexity characteristics of the physiological brain environment. We acknowledge that since our hMGLs are cultured in isolation, in the absence of neurons and astrocytes, and in two-dimensional cultures, their inflammatory response and morphology may be altered (Baxter et al. 2021). Future work should include studies with hMGLs transplanted into rodent brains or organoid models. Moreover, understanding the interaction of *SORL1* with other AD risk factors in regulating microglial lysosome function will further capture the complexity of AD. Nevertheless, our hiPSC model system has enabled a detailed investigation and provided evidence of the cell autonomous role of *SORL1* in regulating microglial lysosome function.

Author Contributions

Conceptualization: S.M., J.E.Y., and S.J. Experimental methodology: S.M., N.M., S.B.S., and C.K. Writing, original draft: S.M. and J.E.Y. Writing, reviewing and editing: S.M., N.M., B.S., S.J., and J.E.Y. Funding acquisition: S.M., N.M., B.S., and J.E.Y.

Acknowledgments

We acknowledge members of the Young and Jayadev laboratories for helpful critiques and discussions of this work. We also acknowledge Dr. Anna Kane in the Stevens lab for critical reading and editing of the manuscript.

Conflicts of Interest

The authors declare no conflicts of interest.

Data Availability Statement

The data that support the findings of this study are available from the corresponding author upon reasonable request.

References

Aiello, A., F. Giannessi, Z. A. Percario, and E. Affabris. 2020. "An Emerging Interplay Between Extracellular Vesicles and Cytokines." *Cytokine & Growth Factor Reviews* 51: 49–60. https://doi.org/10.1016/j.cytogfr.2019.12.003.

Akiyama, H., H. Mori, T. Saido, H. Kondo, K. Ikeda, and P. L. McGeer. 1999. "Occurrence of the Diffuse Amyloid β-Protein (Aβ) Deposits With Numerous Aβ-Containing Glial Cells in the Cerebral Cortex of Patients With Alzheimer's Disease." *Glia* 25, no. 4: 324–331.

2023. "2023 Alzheimer's Disease Facts and Figures." *Alzheimer's and Dementia* 19, no. 4: 1598–1695. https://doi.org/10.1002/alz.13016.

Amos, P. J., S. Fung, A. Case, et al. 2017. "Modulation of Hematopoietic Lineage Specification Impacts TREM2 Expression in Microglia-Like Cells Derived From Human Stem Cells." *ASN Neuro* 9, no. 4: 17590914177166. https://doi.org/10.1177/1759091417716610.

Andersen, O. M., N. Bøgh, A. M. Landau, et al. 2022. "A Genetically Modified Minipig Model for Alzheimer's Disease With SORL1 Haploinsufficiency." *Cell Reports Medicine* 3, no. 9: 100740. https://doi.org/10.1016/j.xcrm.2022.100740.

Andrei, C., P. Margiocco, A. Poggi, L. V. Lotti, M. R. Torrisi, and A. Rubartelli. 2004. "Phospholipases C and A2 Control Lysosome-Mediated IL-1β Secretion: Implications for Inflammatory Processes." *Proceedings of the National Academy of Sciences* 101, no. 26: 9745–9750.

Andrews, N. W. 2000. "Regulated Secretion of Conventional Lysosomes." *Trends in Cell Biology* 10, no. 8: 316–321.

Andrews, N. W. 2017. "Detection of Lysosomal Exocytosis by Surface Exposure of Lamp1 Luminal Epitopes." *Methods in Molecular Biology (Clifton, N.J.)* 1594: 205–211. https://doi.org/10.1007/978-1-4939-6934-0_13.

Arighi, C. N., L. M. Hartnell, R. C. Aguilar, C. R. Haft, and J. S. Bonifacino. 2004. "Role of the Mammalian Retromer in Sorting of the Cation-Independent Mannose 6-Phosphate Receptor." *Journal of Cell Biology* 165, no. 1: 123–133. https://doi.org/10.1083/jcb.200312055.

Baxter, P. S., O. Dando, K. Emelianova, et al. 2021. "Microglial Identity and Inflammatory Responses Are Controlled by the Combined Effects of Neurons and Astrocytes." *Cell Reports* 34, no. 12: 108882. https://doi.org/10.1016/j.celrep.2021.108882.

Beeken, J., S. Kessels, J. M. Rigo, Y. A. Alpizar, L. Nguyen, and B. Brône. 2022. "p27(kip1) Modulates the Morphology and Phagocytic Activity of Microglia." *International Journal of Molecular Sciences* 23, no. 18: 10432. https://doi.org/10.3390/ijms231810432.

Blott, E. J., and G. M. Griffiths. 2002. "Secretory Lysosomes." *Nature Reviews Molecular Cell Biology* 3, no. 2: 122–131.

Bolmont, T., F. Haiss, D. Eicke, et al. 2008. "Dynamics of the Microglial/Amyloid Interaction Indicate a Role in Plaque Maintenance." *Journal of Neuroscience* 28, no. 16: 4283–4292.

Braulke, T., and J. S. Bonifacino. 2009. "Sorting of Lysosomal Proteins." *Biochimica et Biophysica Acta (BBA)—Molecular Cell Research* 1793, no. 4: 605–614. https://doi.org/10.1016/j.bbamcr.2008.10.016.

Braulke, T., J. E. Carette, and W. Palm. 2023. "Lysosomal Enzyme Trafficking: From Molecular Mechanisms to Human Diseases." *Trends in Cell Biology* 34: 198–210.

Buratta, S., B. Tancini, K. Sagini, et al. 2020. "Lysosomal Exocytosis, Exosome Release and Secretory Autophagy: The Autophagic- and Endo-Lysosomal Systems Go Extracellular." *International Journal of Molecular Sciences* 21, no. 7: 2576. https://doi.org/10.3390/ijms21072576.

Burgert, T., V. Schmidt, S. Caglayan, et al. 2013. "SORLA-Dependent and -Independent Functions for PACS1 in Control of Amyloidogenic Processes." *Molecular and Cellular Biology* 33, no. 21: 4308–4320. https://doi.org/10.1128/mcb.00628-13.

Campion, D., C. Charbonnier, and G. Nicolas. 2019. "SORL1 Genetic Variants and Alzheimer Disease Risk: A Literature Review and Meta-Analysis of Sequencing Data." *Acta Neuropathologica* 138, no. 2: 173–186.

Cermak, S., M. Kosicek, A. Mladenovic-Djordjevic, K. Smiljanic, S. Kanazir, and S. Hecimovic. 2016. "Loss of Cathepsin B and L Leads to Lysosomal Dysfunction, NPC-Like Cholesterol Sequestration and Accumulation of the Key Alzheimer's Proteins." *PLoS One* 11, no. 11: e0167428. https://doi.org/10.1371/journal.pone.0167428.

Chen, H. J., J. Yuan, and P. Lobel. 1997. "Systematic Mutational Analysis of the Cation-Independent Mannose 6-Phosphate/Insulin-Like Growth Factor II Receptor Cytoplasmic Domain: An Acidic Cluster Containing a Key Aspartate Is Important for Function in Lysosomal Enzyme Sorting." *Journal of Biological Chemistry* 272, no. 11: 7003–7012.

Cui, Y., J. M. Carosi, Z. Yang, et al. 2019. "Retromer Has a Selective Function in Cargo Sorting via Endosome Transport Carriers." *Journal of Cell Biology* 218, no. 2: 615–631. https://doi.org/10.1083/jcb.201806153.

Di Spiezio, A., A. R. Marques, L. Schmidt, et al. 2021. "Analysis of Cathepsin B and Cathepsin L Treatment to Clear Toxic Lysosomal Protein Aggregates in Neuronal Ceroid Lipofuscinosis." *Biochimica et Biophysica Acta (BBA) - Molecular Basis of Disease* 1867, no. 10: 166205.

Dodson, S. E., M. Gearing, C. F. Lippa, T. J. Montine, A. I. Levey, and J. J. Lah. 2006. "LR11/SorLA Expression Is Reduced in Sporadic Alzheimer Disease but Not in Familial Alzheimer Disease." *Journal of Neuropathology and Experimental Neurology* 65, no. 9: 866–872. https://doi.org/10.1097/01.jnen.0000228205.19915.20.

Dolan, M.-J., M. Therrien, S. Jereb, et al. 2023. "Exposure of iPSC-Derived Human Microglia to Brain Substrates Enables the Generation and Manipulation of Diverse Transcriptional States In Vitro." *Nature Immunology* 24, no. 8: 1382–1390. https://doi.org/10.1038/s41590-023-01558-2.

Domingues, N., S. Catarino, B. Cristóvão, et al. 2024. "Connexin43 Promotes Exocytosis of Damaged Lysosomes Through Actin Remodelling." *EMBO Journal* 43, no. 17: 3627–3649. https://doi.org/10.1038/s44318-024-00177-3.

Dou, Y., H.-J. Wu, H.-Q. Li, et al. 2012. "Microglial Migration Mediated by ATP-Induced ATP Release From Lysosomes." *Cell Research* 22, no. 6: 1022–1033. https://doi.org/10.1038/cr.2012.10.

Dundee, J. M., and G. C. Brown. 2024. "The Microglial P2Y(6) Receptor as a Therapeutic Target for Neurodegenerative Diseases." *Translational Neurodegeneration* 13, no. 1: 47. https://doi.org/10.1186/s40035-024-00438-5.

Dundee, J. M., M. Puigdellívol, R. Butler, T. O. J. Cockram, and G. C. Brown. 2023. "P2Y(6) Receptor-Dependent Microglial Phagocytosis of Synapses Mediates Synaptic and Memory Loss in Aging." *Aging Cell* 22, no. 2: e13761. https://doi.org/10.1111/acel.13761.

Eder, C. 2009. "Mechanisms of Interleukin-1β Release." *Immunobiology* 214, no. 7: 543–553.

Fjorback, A. W., M. Seaman, C. Gustafsen, et al. 2012. "Retromer Binds the FANSHY Sorting Motif in SorLA to Regulate Amyloid Precursor Protein Sorting and Processing." *Journal of Neuroscience* 32, no. 4: 1467–1480.

Gardella, S., C. Andrei, L. V. Lotti, et al. 2001. "CD8+ T Lymphocytes Induce Polarized Exocytosis of Secretory Lysosomes by Dendritic Cells With Release of Interleukin-1β and Cathepsin D." *Blood* 98, no. 7: 2152–2159. https://doi.org/10.1182/blood.V98.7.2152.

Gauthier, C., K. El Cheikh, I. Basile, et al. 2024. "Cation-Independent Mannose 6-Phosphate Receptor: From Roles and Functions to Targeted Therapies." *Journal of Controlled Release* 365: 759–772. https://doi.org/10.1016/j.jconrel.2023.12.014.

Haka, A. S., V. C. Barbosa-Lorenzi, H. J. Lee, et al. 2016. "Exocytosis of Macrophage Lysosomes Leads to Digestion of Apoptotic Adipocytes and Foam Cell Formation." *Journal of Lipid Research* 57, no. 6: 980–992. https://doi.org/10.1194/jlr.M064089.

Hamazaki, H. 1996. "Cathepsin D Is Involved in the Clearance of Alzheimer's Beta-Amyloid Protein." *FEBS Letters* 396, no. 2–3: 139–142. https://doi.org/10.1016/0014-5793(96)01087-3.

Hasanagic, M., A. Waheed, and J. C. Eissenberg. 2015. "Different Pathways to the Lysosome: Sorting Out Alternatives." *International Review of Cell and Molecular Biology* 320: 75–101. https://doi.org/10.1016/bs.ircmb.2015.07.008.

Holstege, H., S. J. van der Lee, M. Hulsman, et al. 2017. "Characterization of Pathogenic SORL1 Genetic Variants for Association With Alzheimer's Disease: A Clinical Interpretation Strategy." *European Journal of Human Genetics* 25, no. 8: 973–981. https://doi.org/10.1038/ejhg.2017.87.

Holstege, H., M. W. J. D. Waal, N. Tesi, et al. 2023. "Effect of Prioritized <Em>SORL1</Em> Missense Variants Supports Clinical Consideration for Familial Alzheimer's Disease." medRxiv, 2023.2007.2013.23292622. https://doi.org/10.1101/2023.07.13.23292622.

Hung, C., E. Tuck, V. Stubbs, et al. 2021. "SORL1 Deficiency in Human Excitatory Neurons Causes APP-Dependent Defects in the Endolysosome-Autophagy Network." *Cell Reports* 35, no. 11: 109259.

Ii, K., H. Ito, E. Kominami, and A. Hirano. 1993. "Abnormal Distribution of Cathepsin Proteinases and Endogenous Inhibitors (Cystatins) in the Hippocampus of Patients With Alzheimer's Disease, Parkinsonism-Dementia Complex on Guam, and Senile Dementia and in the Aged." *Virchows Archiv. A, Pathological Anatomy and Histopathology* 423, no. 3: 185–194. https://doi.org/10.1007/bf01614769.

Ireton, K., H. Van Ngo, and M. Bhalla. 2018. "Interaction of Microbial Pathogens With Host Exocytic Pathways." *Cellular Microbiology* 20, no. 8: e12861.

Itagaki, S., P. McGeer, H. Akiyama, S. Zhu, and D. Selkoe. 1989. "Relationship of Microglia and Astrocytes to Amyloid Deposits of Alzheimer Disease." *Journal of Neuroimmunology* 24, no. 3: 173–182.

Iyer, H., K. Shen, A. M. Meireles, and W. S. Talbot. 2022. "A Lysosomal Regulatory Circuit Essential for the Development and Function of Microglia." *Science Advances* 8, no. 35: eabp8321.

Jacobsen, L., P. Madsen, C. Jacobsen, M. S. Nielsen, J. Gliemann, and C. M. Petersen. 2001. "Activation and Functional Characterization of the Mosaic Receptor SorLA/LR11." *Journal of Biological Chemistry* 276, no. 25: 22788–22796.

Jacobsen, L., P. Madsen, S. K. Moestrup, et al. 1996. "Molecular Characterization of a Novel Human Hybrid-Type Receptor That Binds the α2-Macroglobulin Receptor-Associated Protein." *Journal of Biological Chemistry* 271, no. 49: 31379–31383.

Jacquet, R. G., F. González Ibáñez, K. Picard, et al. 2024. "Microglia Degrade Alzheimer's Amyloid-Beta Deposits Extracellularly via Digestive Exophagy." *Cell Reports* 43, no. 12: 115052. https://doi.org/10.1016/j.celrep.2024.115052.

Jaiswal, J. K., N. W. Andrews, and S. M. Simon. 2002. "Membrane Proximal Lysosomes Are the Major Vesicles Responsible for Calcium-Dependent Exocytosis in Nonsecretory Cells." *Journal of Cell Biology* 159, no. 4: 625–635. https://doi.org/10.1083/jcb.200208154.

Keilani, S., Y. Lun, A. C. Stevens, et al. 2012. "Lysosomal Dysfunction in a Mouse Model of Sandhoff Disease Leads to Accumulation of Ganglioside-Bound Amyloid-β Peptide." *Journal of Neuroscience* 32, no. 15: 5223–5236. https://doi.org/10.1523/jneurosci.4860-11.2012.

Kenessey, A., P. Nacharaju, L. W. Ko, and S. H. Yen. 1997. "Degradation of Tau by Lysosomal Enzyme Cathepsin D: Implication for Alzheimer Neurofibrillary Degeneration." *Journal of Neurochemistry* 69, no. 5: 2026–2038.

Knupp, A., S. Mishra, R. Martinez, et al. 2020. "Depletion of the AD Risk Gene SORL1 Selectively Impairs Neuronal Endosomal Traffic Independent of Amyloidogenic APP Processing." *Cell Reports* 31, no. 9: 107719. https://doi.org/10.1016/j.celrep.2020.107719.

Koike, M., H. Nakanishi, P. Saftig, et al. 2000. "Cathepsin D Deficiency Induces Lysosomal Storage With Ceroid Lipofuscin in Mouse CNS Neurons." *Journal of Neuroscience* 20, no. 18: 6898–6906. https://doi.org/10.1523/jneurosci.20-18-06898.2000.

Kreher, C., J. Favret, M. Maulik, and D. Shin. 2021. "Lysosomal Functions in Glia Associated With Neurodegeneration." *Biomolecules* 11, no. 3: 400. https://doi.org/10.3390/biom11030400.

Kuil, L. E., A. López Martí, A. Carreras Mascaro, et al. 2019. "Hexb Enzyme Deficiency Leads to Lysosomal Abnormalities in Radial Glia and Microglia in Zebrafish Brain Development." *Glia* 67, no. 9: 1705–1718. https://doi.org/10.1002/glia.23641.

Kunkle, B. W., B. N. Vardarajan, A. C. Naj, et al. 2017. "Early-Onset Alzheimer Disease and Candidate Risk Genes Involved in Endolysosomal Transport." *JAMA Neurology* 74, no. 9: 1113–1122. https://doi.org/10.1001/jamaneurol.2017.1518.

La Rosa, F., S. Agostini, F. Piancone, et al. 2023. "TREM2 Expression and Amyloid-Beta Phagocytosis in Alzheimer's Disease." *International Journal of Molecular Sciences* 24, no. 10: 8626. https://doi.org/10.3390/ijms24108626.

Lambert, J.-C., C. A. Ibrahim-Verbaas, D. Harold, et al. 2013. "Meta-Analysis of 74,046 Individuals Identifies 11 New Susceptibility Loci for Alzheimer's Disease." *Nature Genetics* 45, no. 12: 1452–1458. https://doi.org/10.1038/ng.2802.

Lancaster, C. E., A. Fountain, R. M. Dayam, et al. 2021. "Phagosome Resolution Regenerates Lysosomes and Maintains the Degradative Capacity in Phagocytes." *Journal of Cell Biology* 220, no. 9: e202005072. https://doi.org/10.1083/jcb.202005072.

Larsen, J. V., and C. M. Petersen. 2017. "SorLA in Interleukin-6 Signaling and Turnover." *Molecular and Cellular Biology* 37, no. 11: e00641-16. https://doi.org/10.1128/MCB.00641-16.

Lee, H., A. J. Aylward, R. V. Pearse 2nd, et al. 2023. "Cell-Type-Specific Regulation of APOE and CLU Levels in Human Neurons by the Alzheimer's Disease Risk Gene SORL1." *Cell Reports* 42, no. 8: 112994. https://doi.org/10.1016/j.celrep.2023.112994.

Lee, J.-J., T. Wang, K. Wiggins, et al. 2024. "Dysregulated Lysosomal Exocytosis Drives Protease-Mediated Cartilage Pathogenesis in Multiple Lysosomal Disorders." *iScience* 27, no. 4: 109293. https://doi.org/10.1016/j.isci.2024.109293.

Levy, S., G. Sutton, P. C. Ng, et al. 2007. "The Diploid Genome Sequence of an Individual Human." *PLoS Biology* 5, no. 10: e254. https://doi.org/10.1371/journal.pbio.0050254.

Liu, T., B. Zhu, Y. Liu, et al. 2020. "Multi-Omic Comparison of Alzheimer's Variants in Human ESC-Derived Microglia Reveals Convergence at APOE." *Journal of Experimental Medicine* 217, no. 12: e20200474. https://doi.org/10.1084/jem.20200474.

Maninger, J.-K., K. Nowak, S. Goberdhan, R. O'Donoghue, and N. Connor-Robson. 2024. "Cell Type-Specific Functions of Alzheimer's Disease Endocytic Risk Genes." *Philosophical Transactions of the Royal Society B* 379, no. 1899: 20220378.

Marwaha, R., and M. Sharma. 2017. "DQ-Red BSA Trafficking Assay in Cultured Cells to Assess Cargo Delivery to Lysosomes." *Bio-Protocol* 7, no. 19: e2571. https://doi.org/10.21769/BioProtoc.2571.

McQuade, A., and M. Blurton-Jones. 2019. "Microglia in Alzheimer's Disease: Exploring How Genetics and Phenotype Influence Risk." *Journal of Molecular Biology* 431, no. 9: 1805–1817. https://doi.org/10.1016/j.jmb.2019.01.045.

McQuade, A., M. Coburn, C. H. Tu, J. Hasselmann, H. Davtyan, and M. Blurton-Jones. 2018. "Development and Validation of a Simplified Method to Generate Human Microglia From Pluripotent Stem Cells." *Molecular Neurodegeneration* 13, no. 1: 67. https://doi.org/10.1186/s13024-018-0297-x.

McQuade, A., Y. J. Kang, J. Hasselmann, et al. 2020. "Gene Expression and Functional Deficits Underlie TREM2-Knockout Microglia Responses in Human Models of Alzheimer's Disease." *Nature Communications* 11, no. 1: 5370. https://doi.org/10.1038/s41467-020-19227-5.

Meyer-Luehmann, M., T. L. Spires-Jones, C. Prada, et al. 2008. "Rapid Appearance and Local Toxicity of Amyloid-β Plaques in a Mouse Model of Alzheimer's Disease." *Nature* 451, no. 7179: 720–724.

Miao, Y., G. Li, X. Zhang, H. Xu, and S. N. Abraham. 2015. "A TRP Channel Senses Lysosome Neutralization by Pathogens to Trigger Their Expulsion." *Cell* 161, no. 6: 1306–1319.

Mishra, S. 2024. "Differential Effects of SORL1 Deficiency on the Endo-Lysosomal Network in Human Neurons and Microglia." *Philosophical Transactions of the Royal Society of London. Series B, Biological Sciences* 379: 20220389.

Mishra, S., A. Knupp, C. Kinoshita, et al. 2023. "Pharmacologic Enhancement of Retromer Rescues Endosomal Pathology Induced by Defects in the Alzheimer's Gene SORL1." *Stem Cell Reports* 18, no. 12: 2434–2450. https://doi.org/10.1016/j.stemcr.2023.10.011.

Mishra, S., A. Knupp, M. P. Szabo, et al. 2022. "The Alzheimer's Gene SORL1 Is a Regulator of Endosomal Traffic and Recycling in Human Neurons." *Cellular and Molecular Life Sciences* 79, no. 3: 162. https://doi.org/10.1007/s00018-022-04182-9.

Monif, M., C. A. Reid, K. L. Powell, K. J. Drummond, T. J. O'Brien, and D. A. Williams. 2016. "Interleukin-1β Has Trophic Effects in Microglia and Its Release Is Mediated by P2X7R Pore." *Journal of Neuroinflammation* 13, no. 1: 173. https://doi.org/10.1186/s12974-016-0621-8.

Nicolas, G., C. Charbonnier, D. Wallon, et al. 2016. "SORL1 Rare Variants: A Major Risk Factor for Familial Early-Onset Alzheimer's Disease." *Molecular Psychiatry* 21, no. 6: 831–836.

Nielsen, M. S., C. Gustafsen, P. Madsen, et al. 2007. "Sorting by the Cytoplasmic Domain of the Amyloid Precursor Protein Binding Receptor SorLA." *Molecular and Cellular Biology* 27, no. 19: 6842–6851. https://doi.org/10.1128/mcb.00815-07.

Oberstein, T. J., J. Utz, P. Spitzer, et al. 2021. "The Role of Cathepsin B in the Degradation of Aβ and in the Production of Aβ Peptides Starting With Ala2 in Cultured Astrocytes." *Frontiers in Molecular Neuroscience* 13: 615740. https://doi.org/10.3389/fnmol.2020.615740.

Olah, M., E. Patrick, A.-C. Villani, et al. 2018. "A Transcriptomic Atlas of Aged Human Microglia." *Nature Communications* 9, no. 1: 539.

Ovesen, P. L., K. Juul-Madsen, N. S. Telugu, et al. 2024. "Alzheimer's Disease Risk Gene SORL1 Promotes Receptiveness of Human Microglia to Pro-Inflammatory Stimuli." *Glia* 73, no. 4: 857–872. https://doi.org/10.1002/glia.24659.

Pan, X. D., Y. G. Zhu, N. Lin, et al. 2011. "Microglial Phagocytosis Induced by Fibrillar β-Amyloid Is Attenuated by Oligomeric β-Amyloid: Implications for Alzheimer's Disease." *Molecular Neurodegeneration* 6: 45. https://doi.org/10.1186/1750-1326-6-45.

Pietilä, M., P. Sahgal, E. Peuhu, et al. 2019. "SORLA Regulates Endosomal Trafficking and Oncogenic Fitness of HER2." *Nature Communications* 10, no. 1: 2340. https://doi.org/10.1038/s41467-019-10275-0.

Pottier, C., D. Hannequin, S. Coutant, et al. 2012. "High Frequency of Potentially Pathogenic SORL1 Mutations in Autosomal Dominant Early-Onset Alzheimer Disease." *Molecular Psychiatry* 17, no. 9: 875–879.

Quick, J. D., C. Silva, J. H. Wong, et al. 2023. "Lysosomal Acidification Dysfunction in Microglia: An Emerging Pathogenic Mechanism of Neuroinflammation and Neurodegeneration." *Journal of Neuroinflammation* 20, no. 1: 185. https://doi.org/10.1186/s12974-023-02866-y.

Ren, X., L. Yao, Y. Wang, L. Mei, and W. C. Xiong. 2022. "Microglial VPS35 Deficiency Impairs Aβ Phagocytosis and Aβ-Induced Disease-Associated Microglia, and Enhances Aβ Associated Pathology." *Journal of Neuroinflammation* 19, no. 1: 61. https://doi.org/10.1186/s12974-022-02422-0.

Ries, M., and M. Sastre. 2016. "Mechanisms of Aβ Clearance and Degradation by Glial Cells." *Frontiers in Aging Neuroscience* 8: 160.

Rogaeva, E., Y. Meng, J. H. Lee, et al. 2007. "The Neuronal Sortilin-Related Receptor SORL1 Is Genetically Associated With Alzheimer Disease." *Nature Genetics* 39, no. 2: 168–177. https://doi.org/10.1038/ng1943.

Scheltens, P., B. De Strooper, M. Kivipelto, et al. 2021. "Alzheimer's Disease." *Lancet* 397, no. 10284: 1577–1590. https://doi.org/10.1016/s0140-6736(20)32205-4.

Scherzer, C. R., K. Offe, M. Gearing, et al. 2004. "Loss of Apolipoprotein E Receptor LR11 in Alzheimer Disease." *Archives of Neurology* 61, no. 8: 1200–1205. https://doi.org/10.1001/archneur.61.8.1200.

Schindelin, J., I. Arganda-Carreras, E. Frise, et al. 2012. "Fiji: An Open-Source Platform for Biological-Image Analysis." *Nature Methods* 9, no. 7: 676–682. https://doi.org/10.1038/nmeth.2019.

Schmidt, V., A. Subkhangulova, and T. E. Willnow. 2017. "Sorting Receptor SORLA: Cellular Mechanisms and Implications for Disease." *Cellular and Molecular Life Sciences* 74, no. 8: 1475–1483. https://doi.org/10.1007/s00018-016-2410-z.

Scott, G. K., H. Fei, L. Thomas, G. R. Medigeshi, and G. Thomas. 2006. "A PACS-1, GGA3 and CK2 Complex Regulates CI-MPR Trafficking." *EMBO Journal* 25, no. 19: 4423–4435.

Sierksma, A., A. Lu, R. Mancuso, et al. 2020. "Novel Alzheimer Risk Genes Determine the Microglia Response to Amyloid-β but Not to TAU Pathology." *EMBO Molecular Medicine* 12, no. 3: e10606. https://doi.org/10.15252/emmm.201910606.

Park, J.-C., S.-H. Han, and I. Mook-Jung. 2020. "Peripheral Inflammatory Biomarkers in Alzheimer's Disease: A Brief Review." *BMB Reports* 53, no. 1: 10–19. https://doi.org/10.5483/BMBRep.2020.53.1.309.

Stalder, M., A. Phinney, A. Probst, B. Sommer, M. Staufenbiel, and M. Jucker. 1999. "Association of Microglia With Amyloid Plaques in Brains of APP23 Transgenic Mice." *American Journal of Pathology* 154, no. 6: 1673–1684.

Sudwarts, A., S. Ramesha, T. Gao, et al. 2022. "BIN1 Is a Key Regulator of Proinflammatory and Neurodegeneration-Related Activation in Microglia." *Molecular Neurodegeneration* 17, no. 1: 33. https://doi.org/10.1186/s13024-022-00535-x.

Suire, C. N., S. O. Abdul-Hay, T. Sahara, et al. 2020. "Cathepsin D Regulates Cerebral Aβ42/40 Ratios via Differential Degradation of Aβ42 and Aβ40." *Alzheimer's Research & Therapy* 12, no. 1: 80. https://doi.org/10.1186/s13195-020-00649-8.

Sun, B., Y. Zhou, B. Halabisky, et al. 2008. "Cystatin C-Cathepsin B Axis Regulates Amyloid Beta Levels and Associated Neuronal Deficits in an Animal Model of Alzheimer's Disease." *Neuron* 60, no. 2: 247–257.

Suzuki, C., J. Yamaguchi, T. Sanada, et al. 2022. "Lack of Cathepsin D in the Central Nervous System Results in Microglia and Astrocyte Activation and the Accumulation of Proteinopathy-Related Proteins." *Scientific Reports* 12, no. 1: 11662. https://doi.org/10.1038/s41598-022-15805-3.

Taipa, R., S. P. das Neves, A. L. Sousa, et al. 2019. "Proinflammatory Andanti-Inflammatory Cytokines in the CSF of Patients With Alzheimer's Disease and Their Correlation With Cognitive Decline." *Neurobiology of Aging* 76: 125–132. https://doi.org/10.1016/j.neurobiolaging.2018.12.019.

Tancini, B., S. Buratta, F. Delo, et al. 2020. "Lysosomal Exocytosis: The Extracellular Role of an Intracellular Organelle." *Membranes* 10, no. 12: 406. https://www.mdpi.com/2077-0375/10/12/406.

Thonberg, H., H.-H. Chiang, L. Lilius, et al. 2017. "Identification and Description of Three Families With Familial Alzheimer Disease That Segregate Variants in the SORL1 Gene." *Acta Neuropathologica Communications* 5, no. 1: 43. https://doi.org/10.1186/s40478-017-0441-9.

Van Acker, Z. P., A. Perdok, M. Bretou, and W. Annaert. 2021. "The Microglial Lysosomal System in Alzheimer's Disease: Guardian Against Proteinopathy." *Ageing Research Reviews* 71: 101444. https://doi.org/10.1016/j.arr.2021.101444.

Verheijen, J., T. Van den Bossche, J. van der Zee, et al. 2016. "A Comprehensive Study of the Genetic Impact of Rare Variants in SORL1 in European Early-Onset Alzheimer's Disease." *Acta Neuropathologica* 132, no. 2: 213–224.

Verma, R., P. Aggarwal, M. E. Bischoff, et al. 2023. "Microtubule-Associated Protein MAP1LC3C Regulates Lysosomal Exocytosis and Induces Zinc Reprogramming in Renal Cancer Cells." *Journal of Biological Chemistry* 299, no. 5: 104663. https://doi.org/10.1016/j.jbc.2023.104663.

Wan, L., S. S. Molloy, L. Thomas, et al. 1998. "PACS-1 Defines a Novel Gene Family of Cytosolic Sorting Proteins Required for Trans-Golgi Network Localization." *Cell* 94, no. 2: 205–216.

Wang, C., B. Sun, Y. Zhou, A. Grubb, and L. Gan. 2012. "Cathepsin B Degrades Amyloid-β in Mice Expressing Wild-Type Human Amyloid Precursor Protein." *Journal of Biological Chemistry* 287, no. 47: 39834–39841. https://doi.org/10.1074/jbc.M112.371641.

Wang, C., M. A. Telpoukhovskaia, B. A. Bahr, X. Chen, and L. Gan. 2018. "Endo-Lysosomal Dysfunction: A Converging Mechanism in Neurodegenerative Diseases." *Current Opinion in Neurobiology* 48: 52–58. https://doi.org/10.1016/j.conb.2017.09.005.

Wang, F., R. Gómez-Sintes, and P. Boya. 2018. "Lysosomal Membrane Permeabilization and Cell Death." *Traffic* 19, no. 12: 918–931.

Whyte, L. S., C. Fourrier, S. Hassiotis, et al. 2022. "Lysosomal Gene Hexb Displays Haploinsufficiency in a Knock-In Mouse Model of Alzheimer's Disease." *IBRO Neuroscience Reports* 12: 131–141. https://doi.org/10.1016/j.ibneur.2022.01.004.

Willnow, T. E., and O. M. Andersen. 2013. "Sorting Receptor SORLA—A Trafficking Path to Avoid Alzheimer Disease." *Journal of Cell Science* 126, no. 13: 2751–2760. https://doi.org/10.1242/jcs.125393.

Yamazaki, H., H. Bujo, J. Kusunoki, et al. 1996. "Elements of Neural Adhesion Molecules and a Yeast Vacuolar Protein Sorting Receptor Are Present in a Novel Mammalian Low Density Lipoprotein Receptor Family Member." *Journal of Biological Chemistry* 271, no. 40: 24761–24768.

Young, J. E., J. Boulanger-Weill, D. A. Williams, et al. 2015. "Elucidating Molecular Phenotypes Caused by the SORL1 Alzheimer's Disease Genetic Risk Factor Using Human Induced Pluripotent Stem Cells." *Cell Stem Cell* 16, no. 4: 373–385. https://doi.org/10.1016/j.stem.2015.02.004.

Young, J. E., L. K. Fong, H. Frankowski, G. A. Petsko, S. A. Small, and L. S. B. Goldstein. 2018. "Stabilizing the Retromer Complex in a Human Stem Cell Model of Alzheimer's Disease Reduces TAU Phosphorylation Independently of Amyloid Precursor Protein." *Stem Cell Reports* 10, no. 3: 1046–1058. https://doi.org/10.1016/j.stemcr.2018.01.031.

Zhang, Y., S. A. Sloan, L. E. Clarke, et al. 2016. "Purification and Characterization of Progenitor and Mature Human Astrocytes Reveals Transcriptional and Functional Differences With Mouse." *Neuron* 89, no. 1: 37–53.

Zhong, D., R. Wang, H. Zhang, M. Wang, X. Zhang, and H. Chen. 2023. "Induction of Lysosomal Exocytosis and Biogenesis via TRPML1 Activation for the Treatment of Uranium-Induced Nephrotoxicity." *Nature Communications* 14, no. 1: 3997. https://doi.org/10.1038/s41467-023-39716-7.

Supporting Information

Additional supporting information can be found online in the Supporting Information section.